Fuel Cell Research

DE-SC0001556

Peter M. Weber, PI

Brown University

Department of Chemistry

Final Report

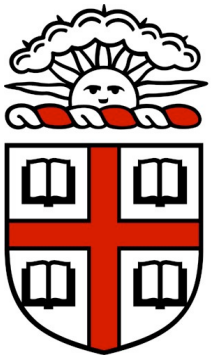

Executive Summary

In conjunction with the Brown Energy Initiative, research Projects selected for the fuel cell research grant were selected on the following criteria:

- They should be fundamental research that has the potential to significantly impact the nation's energy infrastructure.
- They should be scientifically exciting and sound.
- They should synthesize new materials, lead to greater insights, explore new phenomena, or design new devices or processes that are of relevance to solving the energy problems.
- They involve top-caliper senior scientists with a record of accomplishment, or junior faculty with outstanding promise of achievement.
- They should promise to yield at least preliminary results within the given funding period, which would warrant further research development.
- They should fit into the overall mission of the Brown Energy Initiative, and the investigators should contribute as partners to an intellectually stimulating environment focused on energy science.

Based on these criteria, fourteen faculty across three disciplines (Chemistry, Physics and Engineering) and the Charles Stark Draper Laboratory were selected to participate in this effort.[1] In total, there were 30 people supported, at some level, on these projects. This report highlights the findings and research outcomes of the participating researchers.

[1] Prof. Sweigart has passed away; no report is made on the outcome of his research.

DOE Fuel Cell Research Grant
Final Progress Report
PI: Peter M. Weber

Table of Contents

Bernskoetter, Wesley H.

Azerovalent molybdenumcomplex, $[(Ph_2PCH_2CH_2)_2PPh]Mo(C_2H_4)(N_2)_2$, was found to promote coupling of CO_2 and ethylene to afford a molybdenum(II) acrylate hydride complex. The identity of the molybdenum(II) acrylate hydride complex was established by spectroscopy and reactivity studies. The mechanism of carbon dioxide functionalization with ethylene has been investigated by a series of kinetic and isotopic labeling studies, in addition to the observation of a formally molybdenum(0) carbon dioxide-ethylene intermediate along the reaction pathway. Acrylate formation from the molybdenum(0) intermediate proceeds with a rate constant of $3.8(3) \cdot 10^{-5}$ s^{-1} and an isotope effect of 1.2(2) forC_2H_4 vs. C_2D_4 at 23 °C. Measuring rate constants of the CO_2 reduction over a 40 ° C temperature range established activation parameters for acrylate formation of $\Delta S^{\ddagger} = 1(7)$ eu and $\Delta H^{\ddagger} = 24(3)$ kcal/mol. The mechanism of CO_2-ethylene coupling is proposed to proceed from a molybdenum(0) carbon dioxide-ethylene adduct via rate-limiting oxidative C-C bond formation followed by rapid β-hydride elimination from a metallalactone complex.

Calo, J.M.

DEVELOPMENT OF A HYDRODYNAMIC DIRECT CARBON FUEL CELL (H/DCFC)

The use of solid carbonaceous fuels for power generation and/or carbonaceous waste management in a robust and efficient manner has a large number of potential applications in the general area of environmentally benign energy generation. One possible, fruitful direction in this regard is the development of a robust direct carbon fuel cell (DCFC) that can generate power without combustion. DCFCs offer a number of potential benefits in this regard, beginning with the highest theoretical efficiency of any known fuel cell type. However, the fact that the fuel is solid rather than fluid creates a number of significant challenges that have not yet been satisfactorily solved. This is essentially the "real world" problem addressed by this research project – namely, the development of a robust DCFC that can deal effectively with these problems – in our case, the hydrodynamic, direct carbon fuel cell (H/DCFC).

Methodology

The direct carbon fuel cell (DCFC) can be used to generate electrical power from almost any carbonaceous fuel, including coal, biomass, and organic waste, making it an attractive option for simultaneous power generation and carbonaceous waste management. One of the primary motivations in this regard is the high theoretical efficiency of the DCFC, which when measured as $\eta = \Delta G/\Delta H$ for carbon oxidation, exceeds 100% - greater than any other known fuel cell.

In spite of potentially attractive benefits, DCFC technology still requires additional development before it can become a commercially feasible option for power generation and waste carbon management. Some significant problems that must be addressed include technology for continuous fueling of cells, maintaining, cleaning and recycling the electrolyte, minimization of fuel "corrosion" (i.e., thermal losses of carbon fuel), plus a number of other related problems, including those that are common to other high temperature fuel cells.

The hydrodynamic direct carbon fuel cell (H/DCFC) that is under development in this project specifically addresses a number of these important issues. It is based on the application of recirculating slurry of carbonaceous fuel particles in a molten hydroxide

electrolyte. Continuous slurry circulation is accomplished *via* "gas-lift" with an inert gas. The recirculating slurry is used to continuously deliver fuel to the anode surfaces and to remove fuel ash. The electrolyte can be continuously cleaned of ash in an external circulation loop using well-known aqueous phase treatment methods. In addition, the lift-gas purges the cell such that it can be used to control CO_2 levels to minimize carbon corrosion, and/or produce highly concentrated CO_2 for effective direct sequestration or chemical conversion to other products.

Significant progress has been made in the development of a H/DCFC. Using a novel batch DCFC as a "test bed," we have successfully developed various elements of the continuous H/DCFC, such as a rectangular anode and cathode that are effective and robust, and are capable of "stacking" in order to increase the total voltage and power over that from a single cell. We have also focused on the issue of developing techniques to decrease the effective operating temperature of the fuel cell in order to extend fuel cell life and minimize fuel (carbon) losses due to corrosion. We have also explored issues related to the molten electrolyte and the performance of various different carbonaceous fuels in the DCFC.

Some of the preceding issues have been reported in a series of papers based on this work:

1. Guo, L, Calo, JM, DiCocco, E, Bain, EJ. Development of a low temperature, molten hydroxide direct carbon fuel cell. *Energy & Fuels*, 2013, 27 (3), 1712–1719.
2. Guo, L.; Calo, J.M.; Kearney, C.; Grimshaw, P. The anodic reaction zone and performance of different carbonaceous fuels in a batch molten hydroxide direct carbon fuel cell. *Appl. Energy,* 2013, submitted, in review.
3. Grimshaw, P.; Calo, J.M.; Liang, G.; Podhoretz, S. Wetting of carbonaceous fuel particles by molten alkali metal hydroxide and carbonate electrolytes. *Energy & Fuels,* 2014, DOI 10.1021/ef4024004.

It is also noted that a patent application has been filed on this work and the attendant concepts.

Doll, Jimmie D.

Summary

Our research is an investigation that involves the development and application of novel Monte Carlo algorithms. These methods are designed to cope with the "rare-event" sampling problem, a ubiquitous issue associated with the numerical simulation of thermally activated processes in complex physical, chemical and biological systems.

Results

The work supported by our portion of the Fuel Cell award reinforces our efforts in a larger, collaborative project funded by DOE ("Large Deviation Methods for the Analysis and Design of Monte Carlo Schemes in Physics and Chemistry," DOE award DE-SCOO02413, (Brown Portion: $758,659, Los Alamos Portion: $513,358), 1/01/09 – 12/31/11), involving researchers from Applied Mathematics at Brown (Professors Paul Dupuis and Hui Wang) and from Los Alamos National Lab (J. Gubernatis).

Funding from the Fuel Cell Research grant has made it possible to attract Swiss National Science Foundation Postdoctoral Fellow Nuria Plattner to Brown for two years, offering partial support for her during 2010 to supplement her Swiss award that will support her for 2011. Dr. Plattner has completed the first of a series of studies that demonstrate that our newly developed methods represent a substantial advance over currently available methods.

Kim, Eunsuk

Our laboratory has developed synthetic modeling systems of formate dehydrogenases in order to achieve efficient transformation between CO_2 and formic acid. Formic acid is a currently used fuel for a fuel cell and is oxidized to CO_2 at the anode. One of the challenges in the practical use of formic acid fuel cells is the high overpotential. Our research goal is to overcome this challenge by adapting the chemical principles of natural enzymes into the synthetic catalysts. Formate dehydrogenase (FDHs) are enzymes that catalyze the two electron oxidation of formate (HCO_2^-) to CO_2 coupled to the reduction of $NAD(P)^+$ to NAD(P)H.[1] In some prokaryotes, the FDHs contain molybdenum (Mo) or tungsten (W) cofactors, by which an efficient CO_2-reductase activity (reduction of CO_2 to formate) as well as formate dehydrogenase activity (oxidation of formate to CO_2) has been observed. In 2008, Hirst and coworkers have shown that a purified W-FDH can activate an electrode to catalyze reversible oxidation of formate to CO_2 more efficiently than any of known synthetic catalysts.[2] Despite the promise shown in electrocatalytic activity of the FDH enzyme, the efforts in synthetically imitating FDH's function is currently lacking in the field.

With the support of the DOE Fuel cell project, our laboratory has prepared a group of biomimetic Mo/W complexes that share the primary coordination environment with that of FDHs.[4] The FDHs utilize a bis(dithiolene) bound M^{IV} (where M = Mo or W) for the catalysis. The use of high-valent metal ions with non-innocent ligands by the enzyme is a very different strategy from the most known synthetic catalysts in which the metal ions in much lower valences, 0, +1, and +2, are typically used.[3] With systematically varied biomimetic complexes and the corresponding reactivity studies, we have learned that both the primary as well as the secondary coordination environment play the critical roles for the formate/CO_2 transformation.[4] In a different study, we also have investigated reaction chemistry that is needed to regenerate the active metal for the efficient turnover of the catalytic site.[5]

(1) Hille, R. *Chem Rev* **1996**, *96*, 2757-2816.

(2) Reda, T.; Plugge, C. M.; Abram, N. J.; Hirst, J. *Proc Natl Acad Sci USA* **2008**, *105*, 10654-8.

(3) Gibson, D. H.: *Chemical Reviews* **1996**, *96*, 2063-2095.

(4) Seo, J.; Kim, E. *Inorg. Chem.* **2012**, *51*, 7951-7953.

(5) Seo, J.; Williard, P. G.; Kim, E. *Inorg. Chem*. **2013**, *52*, 8706-8712

Marston, J. Bradley

Summary:

We have simulated model systems that can rectify optical-frequency electric fields, with the ultimate goal of finding a new way to directly convert sunlight to electricity. The modeled devices consist of a junction of a Mott insulator or highly correlated metal with an ordinary band metal. Such devices could be made by nanofabrication techniques, allowing experimental validation of the idea.

Details:

We have investigated junctions built around doped Mott insulators as novel ways to construct rectifying devices that function at extremely high frequencies (order 100 THz). A t-V model of spinless electrons moving in one spatial dimension demonstrates that electron-electron interactions are crucial for rectification. We are currently extending the analysis in several ways: to dissipative systems, to realistic spinning electrons, to multichannel models, and to longer systems. These models, while conceptually simple, offer rich physical insight into contrasting single photon versus collective electric field driven processes, and the practical possibilities for applications such as optical harmonic generation and hybrid rectennas to harvest solar energy.

Pacifici, Domenico

Summary:

With investigate the use of nanopatterned metal films to enhance electromagnetic field intensity and light absorption in thin film photovoltaics. The aim of the work is to generate "plasmonic concentrators" for efficient light harvesting.

To this end, we designed, fabricated and characterized several hole arrays milled in silver films and distributed according to various periodic and quasiperiodic tilings of the plane. Preliminary results show a broadband absorption enhancement in 24-nm thick P3HT:PCBM polymer films by using nanopatterned metal films as planar concentrators of the incident light. The absorption enhancement is caused by increased electromagnetic fields at the metal/absorber interface, as the result of light scattering into propagating surface plasmon polaritons. By properly designing the position of the holes in the metal film, we were able to achieve broad-band, polarization-insensitive absorption in an ultra-thin absorber.

Palmore, G. Tayhas

Our initial project supported research on polymer-based batteries where issues related to the stability of the cathode material to repetitive cycling were addressed. The results of this study were reported in *Electrochemistry Communications* **2010**, *12*, 761 (Sung Yeol Kim, Sujat Sen, Hyun-Kon Song, G. Tayhas R. Palmore) and are summarized below in Project 1. The studies of Project 1 led to a discovery that electrocrystallization of dopant impacts the properties of the polymer composite (e.g., conductivity, porosity) used in the polymer-based batteries. This phenomenon was examined more closely and the results, which are summarized below in Project 2, have been submitted for publication. In addition, we have capitalized on our previous work with bioelectroactive materials for oxygen reduction and coupled these materials with a photoanode of rutile TiO_2 to yield an "artificial leaf". This work has been submitted for publication and is summarized below in Project 3. Finally, we have initiated studies on the mechanical stress in conducting polymers during voltage excursions. These studies were initiated for the purpose of understanding delamination phenomenon between ion-conducting polymers and electrode surfaces. This work represents the first of its kind and results from these studies have implications for all ionic polymers, including those used in fuel cells. This work is in progress and is summarized in Project 4.

Project 1. *Enhancing the stability and performance of a battery cathode using a non-aqueous electrolyte.* For conductive polymers to be considered materials for energy storage, both their electroactivity and stability must be optimized. In this study, a non-aqueous electrolyte (0.2 M $LiClO_4$ in acetonitrile) was studied for its effect on the charge storage capacity and stability of two materials used in batteries developed in our laboratory, polypyrrole (pPy) and poly(3,4-ethylenedioxythiophene) (PEDOT) doped with 2,2′-azinobis(3-ethylbenzothiaxoline-6-sulfonic acid (ABTS). The results are compared to the performance of these materials in an aqueous electrolyte (0.2 M HCl/aq). Loss of ABTS dopant was eliminated principally due to the low solubility of ABTS in acetonitrile, resulting in cathode materials with improved stability in terms of load cycling and performance.

Project 2. *Effect of polymerization potential and electrocrystallization of dopant on the*

properties of electrosynthesized films of PEDOT[ABTS]. Investigating the effect of synthetic conditions on the properties of conducting polymers (CPs) is a prerequisite to the success of using these materials in new technologies. In this study, films of poly(3,4-ethylenedioxythiophene) (PEDOT) doped with 2,2'-azino-bis(3-ethylbenzothiaxoline-6-sulfonic acid) diammonium salt (ABTS) were electrosynthesized over a range of potentials to determine the effect that polymerization potential has on the properties of PEDOT[ABTS] films. It was found that increasing the polymerization potential from 1.2V to 1.8V prevented electrocrystallization of the ABTS dopant, which resulted in better quality films with respect to adhesion, interconnected morphology, electroactivity and conductivity. This study demonstrates the important role that dopants and polymerization conditions have on the properties of electrosynthesized CPs, especially when dopants with added functionality (i.e., redox, biological, or catalytic activity) are used.

Project 3. *An Artificial Leaf that Generates Electricity: Coupling Photoelectro-oxidation of Water to Bioelectro-reduction of Oxygen.* In this study, we demonstrate energy conversion in a device that couples photo- and bioelectrocatalysis. This device can be described as a photoelectrochemical biofuel cell where fuel is supplied via Fujishima-Honda-type photoelectrolysis of water. The overall reaction of this system is the reversible interconversion of oxygen and water. A photoanode of TiO_2 (rutile, single crystal) splits water into O_2 when illuminated, providing an internal substrate (i.e., cathodic fuel) for the oxidoreductase, laccase. The cathode of this system consists of an electrode coated with a conducting polymer matrix entrapping laccase and a redox mediator, 2,2'-azino-bis(3-ethylbenzothiaxoline-6-sulfonic acid (ABTS) (PAL-coated cathode), previously reported by our laboratory. The immobilization of the enzyme and its mediator eliminates the need for a separation membrane, allowing the anode and cathode to be located in the same compartment.

Project 4. *In-situ measurement of mechanical stress in conducting polymers during electrochemical cycling.* We report the profiles of stress incurred within a polypyrrole film doped with IC (pPy[IC]) when the film was subjected to electrochemical potential cycling. To investigate the effects of electrolyte on the stress profile, several different electrolytes were employed. We have analyzed the ion transport in the conducting

polymer film for each electrolyte, which has begun to reveal a physical/chemical mechanism to describe the break-in period for conductive polymers.

Rose-Petruck, Christoph

The goal of the project was to provide fundamental insight into the physical processes during gas trapping and release as well as engineering-oriented data useful for the design of a gas storage systems and fuel cells. To this end, ultrafast structural measurements of the clathrates were carried out. Data, such as gas storage capacity and gas loading and unloading rates are measured in a separate, specifically designed batch process chamber. Furthermore, x-ray imaging techniques directly relevant to the characterization of fuel cell and battery electrodes are developed.

Two projects were explored:

1) Two machines for the production of clathrate hydrates were constructed. Measurements of the CO_2 uptake have begun using a closed circulation systems that can be pressurized. The uptake has so far been rather low because of the formation of a clathrate layer on top of the water. This layer inhibits the diffusion of CO_2 into the water for further clathrate formation. The machine is currently modified with a continuous stirring mechanism to prevent this effect. The second machine can not be pressurized but instead forms clathrates though a mixture of water and THF. This machine can produce clathrate that have been successfully circulated to the ultrafast x-ray imaging instrument.

2) A novel x-ray imaging techniques, called Spatial Frequency X-ray Heterodyne Imaging (SFXHI), has been used. It permits the x-ray image formation based on the x-radiation scattered off the sample. Since the intensity of the scattered radiation is directly related to the structure of materials and does not rely on the absorption of x-rays, it can be used for imaging in situations where the x-ray absorption does not change or is negligible to begin with. The technique has been demonstrated to distinguish between water and water-ice slurries, delivering a contrast that is one to two orders of magnitude larger than the absorption contrast. SFXHI can also be used for imaging the structure of electrodes of secondary batteries or fuel cells. It is desirable for catalysts and battery electrodes alike to maintain a highly disperse (nano-) structure in order to maximize the reactive surface area and reaction rate. We have demonstrated that SFXHI can produce images of nanoparticles distributions of carbon, gold, and other metals. A first test imaging application has been tried in late March 2011 at ID7 of the Advanced Photon Source. A

Li-polymer battery was imaged during the charging and discharging cycle with the goal to observe the magnate oxidation at the cathode during charging and the accompanying cathode "swelling". The data that resulted did not show a structure change of the electrodes during discharge

The DOE support resulted in a patent disclosure that has been filed with the Brown Technology Ventures Office on the release of CO_2 from clathrates using ultrasound.

No publications were published as a direct result of this support. However, the DOE-supported work laid the foundation for a clathrate research program that resulted in 2013 in our participation in a successful application to the National Science Foundation for the funding of a Phase I Center for Carbon Capture and Conversion. Based on the experience we gained during our DOE-supported work we built a new version of a clathrates reactor. This reactor is now used in the electrochemical and homogeneous catalytic conversion of CO_2 to feedstock (C2, C3, C4 alkanes and alkenes, and formic acid) useful for the chemical industry. The goal of this research is the reduction of dependency of the chemical industry on mineral oil feedstock.

Sello, Jason K.

Research focused on the chemical capture of carbon dioxide and the conversion of plant biomass into fuels. Both of these areas are inspired by microbial metabolism. One project involves the capture of carbon dioxide using small molecule mimics of methanofuran, a co-factor used by methanogenic Archaea for the capture and consumption of carbon dioxide. The second project involves the use of *Streptomyces* bacteria for the conversion of the carbon in plant biomass into triglyceride precursors of biodiesel.

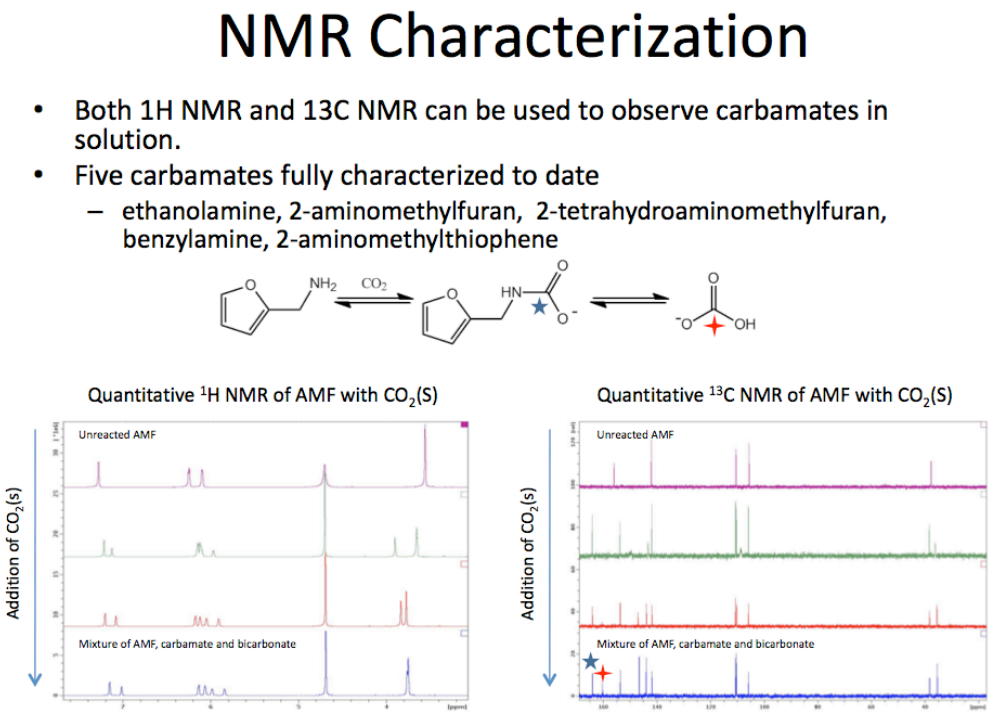

Our efforts to capture carbon dioxide are inspired by the ability of organisms called Archaea to generate methane from carbon dioxide. These organisms use a biological co-factor called methanofuran for the capture of atmospheric carbon dioxide. This co-factor has an aminomethylfuran structure that spontaneously reactions with carbon dioxide yielding a stable carbamate product. To understand the chemistry of this peculiar functionality, we are synthesizing derivatives of aminomethylfurans that we hypothesized will have enhanced capability to capture carbon dioxide. In a series of preliminary studies, we compared the reactivity of aminomethyl furan with four closely related structures. Using quantitative 1H NMR and 13CNMR, we have made measurements of the relative reactivities of these compounds. Thus far, we have found there to be very

little difference in reactivity between these compounds. However, we have found that the aminomethyl furan promotes the rapid conversion of carbon dioxide (dissolved in water) into bicarbonate (please see data above). This unanticipated observation is quite interesting and has implications for the capture and conversion of carbon dioxide. Based on this finding, we are now investigating the capacity of amino methyl furan derivatives and other amines to promote the hydration of carbon dioxide. We are planning a manuscript that outlines these interesting findings.

On a separate project but related project, we examined the ability of *Streptomyces* bacteria to convert the lignin component of plant biomass into triglycerides. These bacteria have the ability to convert lignin derived aromatic compounds into acetyl coenzyme A and succinyl coenzyme A. Acetyl coenzyme A is the biochemical precursor of triglycerides. To determine if the carbon of a lignin derived aromatic compound is incorporated into triglycerides, we have been been feeding *Streptomyces coelicolor* (a model organism) ^{13}C-labelled aromatic compounds. Consistent with our hypothesis, we have observed the incorporation of the radiolabel into the triglycerides. These findings suggest that these organisms can be used for the conversion of plant biomass components into a biofuels precursor.

Stein, Derek

Project summary:

Ion transport through nanoporous membranes plays a crucial role in energy technologies that include batteries, fuel cells, and novel energy harvesting devices. It has been theoretically predicted that the efficiency of these technologies can be significantly enhanced, by orders of magnitude in some cases, by obtaining a high surface charge density and promoting hydrodynamic slip at the solid-liquid interface. This project sought to control the solid-liquid interface and understand the interplay between the surface charge density and the occurrence or absence of hydrodynamic slip there.

Results:

We developed fluidic devices, including nanochannels and nanopores, which model the pores of an ion-selective membrane. Our devices have highly controlled geometries that are easy to model theoretically. Their surfaces are charged in solution. The main outcome of our work was to develop a method of controlling that charge electrically.

One can modulate the surface charge density at the solid-liquid interface using a fluidic version of the field-effect. The electric charge on an electrode located beneath the surface of an insulating dielectric influences the electrochemical potential within a thin layer of the fluid above. We use the term "electrofluidic gating" to describe such voltage-actuated control over the electric double layer. We have modeled this effect theoretically, developed fabrication techniques to realize electrofluidic devices, and demonstrated control over the selective ionic conductance of a single nanopore. In particular, we were able to exert control over the surface charge density of a nanopore, and hence its conductance and selectivity. We observed no evidence of hydrodynamic slip, however, possibly because it is fundamentally incompatible with high surface charge densities, and possibly because it requires a special material at the solid-liquid interface. Our results were reported in the papers listed below.

Related publications:

1. "Electrofluidic Gating of a Chemically Reactive Surface", Zhijun Jiang and Derek Stein, *Langmuir* **26**, 8161-8173 (2010).

2. “Fabrication of nanopores with embedded annular electrodes and transverse CNT electrodes”, Zhijun Jiang, Mirna Mihovilovic, Jason Chan, and Derek Stein, Journal of Physics: Condensed Matter **22**, 454114 (2010).
3. “Charge Regulation in Nanopore Ionic Field-Effect Transistors”, Zhijun Jiang and Derek Stein, *Physical Review E* **83**, 031203 (2011).

Sun, Shouheng

We have synthesized monodisperse core/shell Au/CuPt nanoparticles by co-reduction of platinum acetylacetonate and copper acetylacetonate in the presence of Au nanoparticles. The CuPt alloy effect and core/shell interactions make these Au/CuPt nanoparticles promising catalyst for both oxygen reduction reaction and methanol oxidation reaction. Our studies show that the existence of Au nanoparticle core not only minimizes the Pt usage, but also improves the stability of the Au/CuPt catalyst for fuel cell reactions.

Suuberg, Eric

Measurement and Prediction of Thermodynamic Properties of Candidate Gasification/Reforming Fuels

One of the many issues facing engineers designing fuel conversion systems is the absence of thermodynamic property data on many new candidate fuel materials. With increasing use of low-quality feedstocks for advanced conversion devices feeding fuel cells (such as gasifiers or reformers), it becomes important to learn more about such materials. This project has a goal of both measuring, as well as developing methods for predicting, key thermodynamic properties of heavy organics.

Heavy oils, shale oils, heavy residues of biomass conversion processes are all candidate materials for the gasification or reforming front end of fuel cell devices. These fuels are in and of themselves unattractive in most advanced energy conversion concepts. They cannot be fed to gas turbines because they are viscous liquids or semi-solids. They have low hydrogen to carbon ratios, so they cannot be cracked with any significant yields to lighter fuels of greater value. They can be burned in equipment for solids or heavy oil combustion, but this is generally associated with a steam turbine cycle in order to capture the work value. Hence, some kind of gasification or reforming-type of scheme is an attractive option for producing a hydrogen stream that upon water-gas shifting and purification, could feed a fuel cell. There are many possible process concepts. A key design variable for some would be the vapor pressure of these materials. This project has been engaged in measuring the vapor pressures of these tarry-like materials (mixtures of high molecular weight organics). A significant number of results have been obtained on pure compounds and their mixtures. Such measurements are, however, tedious and difficult, given the nature of the materials. Because of this, we have explored the use of quantum-chemical based estimation techniques for predicting vapor pressures. One particular technique of interest involves use of the conductor-like screening model for realistic solvation (COSMO-RS). Because actual prediction of thermodynamic properties of mixtures of large molecules using *ab initio* techniques is computationally prohibitive, the approach being pursued involves optimizing the electronic structure of the molecules of interest in a detailed quantum mechanical calculation, but then using a simplified

approximation to the charge density distribution over a molecular surface to predict interactions with neighboring molecules in a mixture. This approach does not require the purely empirical establishment of group additivity contributions, as some presently popular estimation methods entail. On the other hand, it is computationally tractable enough to run on desktop computing environments. We have achieved some success in a prediction of some key properties of fairly large aromatic compounds, but still need to establish why the technique begins to fail for larger species.

Weber, Peter M.

Structure-specific molecular detection

Summary

A common challenge for the research projects that are part of the fuel cell collaboration is the detection of molecules, preferentially in a time-resolved manner, that is specific to molecular structures. Our research project develops such an enabling technology and explores applications in multiple arenas. The work directly interfaces to the projects of Profs. Marston and Pacifici that are described elsewhere in this report.

Results:

We have discovered that Rydberg states are ideal reporters of the molecular structure. The structure sensitivity can be understood based on the phase shift that electrons experience when passing a positively charged ion core. The phase shift depends sensitively on the spatial location of all the charges that make up the molecule. Its measurement, which in traditional experiments is performed by electron or x-ray diffraction, is conveniently done by reading out the energy of the Rydberg levels. The experiment can be implemented both in a molecular beam or in atmospheric pressure gases.

In the laboratory, we have implemented the technique on several interesting systems of molecular dynamics. One example is 1,4- diazabicyclo[2.2.2]octane (DABCO), for which we have measured the time dependent structural dynamics. DABCO and similar strained multi-ring molecules can play important roles as energy carriers. The theoretical modeling of the experiment involves the calculation of the potential energy surfaces and subsequent optimization of the Rydberg electron wave function. The close coordination of experimental and computational work enabled rapid progress that led to significant advances in detection technology.

Final Report to Brown University Charles Stark Draper Laboratory

DOE Award number: DE-SC0001556

Subaward number: 00000355

prime recipient: Brown University

subawardee: The Charles Stark Draper Laboratory

subawardee program manager: Michael Y. Feng

project title: Fuel Cell Research

Executive Summary

The Charles Stark Draper Laboratory (Draper) worked on three separate energy projects in collaboration with Brown University. The first project in collaboration with Professor Christoph Rose-Petruck (chemistry) investigated new novel approaches to low cost utility-scale energy storage. The second project in collaboration with Professor Joe Calo (engineering) furthered the development of a direct carbon fuel cell. The third and final project in consultation with Professors Tayhas Palmore (engineering), Shouheng Sun (chemistry), and Christoph Rose-Petruck (chemistry) built and tested a small scale rechargeable zinc air battery. Roughly 50% of the effort was expended on the DCFC while the remaining 50% was split between energy storage and the rechargeable zinc air battery. Brief descriptions of the three projects follow.

ENERGY STORAGE

As more renewable energy sources are deployed on the nation's grid, utility-scale energy storage will be needed to ensure customer power demands are met despite the random availability of renewable power. Currently, energy storage is accomplished by pumping water against gravity, flywheels, and electrochemical batteries, but these have not been widely adopted.

This project explored three concepts for storing energy on a utility-scale at low cost. The first concept uses clathrate hydrates to more efficiently compress gases for energy storage. The second concept examined if the equipment for carbon capture sequestration (CCS) could be used for energy storage. An economic model showed

that this was economically feasible if the capital cost of the CCS equipment was already included. For a 10^4 m^3 tank pressurized to 15 MPa, there would be 90 MW-hr of storage.

The last concept for energy storage was to convert already existing large bodies of water such as a power plant's cooling pond or lake into an electrochemical battery. It was assumed the body of water could be converted into a copper-zinc battery with a porous disk in the middle to separate the anode from the cathode. If this were possible, the volume in a cooling pond or water reservoir could store anywhere from 10 GW-hr to 23 TW-hr.

DIRECT CARBON FUEL CELL

Direct Carbon Fuel Cells (DCFC) react carbon and oxygen electrochemically to generate electrical power with near 100% thermodynamic efficiency. The technology has limited moving parts. Even when supporting equipment and resistive losses are included, a DCFC system could operate close to 60% efficiency. This would cause fuel costs and carbon dioxide emission reductions of 50% over conventional coal fired power plants. Electrical power generation would be less expensive with a reduced carbon footprint. A DCFC can also operate using any high carbon fuel source, which gives utility in a host of other applications including remote power generation and even organic waste removal.

This project was targeted at studying the system level advantages and limitations of DCFC technology. As a result, this program produced a system level DCFC design and model with an efficiency of 54% operating at a current density of 18 mA/cm^2. The design includes a fuel pyrolyzer and electrolyte circulation system that enable long term continuous operation. Efficiency calculations were derived from a detailed system level thermodynamic model incorporating fuel pyrolysis, phase changing material flow, heat exchangers, conductive heat loss, internal resistance, electrolyte vaporization, carbonate formation, and the Reverse Boudouard reaction.

Achieving this performance required several unique engineering developments. First, lift gas ports were used to transport the carbon/hydroxide slurry through a tortuous path in the anode chamber. This allows for a single-pass, continuous flow, fuel cell capable of removing ash and processing contaminated electrolyte. Second, a steam management system was designed to efficiently generate the steam required for lift gas supply and cathode reaction support. By transferring heat between condensing and vaporizing processes, this provided steam flow and separation for minimal energy cost.

Despite promising efficiency levels, this report also revealed and re-verified multiple practical issues with implementing DCFC technology in a commercially viable system. Sensitivity analysis showed that even minor levels of carbonate production will cause significant practical and economic issues with deployment. Carbonate production requires additional sodium hydroxide electrolyte to be continuously fed into the system as a consumable. The cost and logistics of supplying sodium hydroxide make this technology ineffective compared to combustion-based alternatives. Carbonate production may be preventable with high

concentrations of steam in the anode chamber, but further experimental testing is required.

System modeling also demonstrated that current experimentally measured cell resistance values are unacceptable. The baseline system studied in this report produced a maximum power output of 67 kW. At this power level, the cell stack alone measures 2.5' x 4' x 9' weighing nearly 20 tons. Capital costs would be orders of magnitude greater than existing combustion-based systems, such as portable diesel generators. It has been demonstrated that electrode spacing has a significant impact on cell resistance. Reducing electrode spacing combined with increasing the active area should be a key focus area in the future.

Finally, materials testing verified that advanced materials or coatings will be required beyond typical metals. Both anode and cathode electrodes require an electrically conductive surface that is highly corrosion resistant to sodium hydroxide and elevated temperature. Solid nickel performed moderately well over 24 hours; however, un-sintered nickel mesh samples suffered from rapid rates of oxidation and deterioration. It is suspected that conductive ceramics may be the only viable option. Several candidates such as zirconium nitride and chromium nitride are currently being explored.

RECHARGEABLE ZINC AIR BATTERY

Currently, lithium ion batteries dominate the rechargeable battery market. However, lithium is in limited supply in the U.S. and must generally be imported; in addition, a fire hazard exists with lithium. On the other hand a Zn-air battery uses materials in much greater supply in the U.S. and is far safer. However, the inability to recharge a Zn-air battery is a major limiting factor. The problem is related to CO_2 in the air which poisons the electrolyte (converts KOH to K_2CO_3) and therefore renders them primary (non-rechargeable) designs.

Draper designed a cell that utilizes a quaternary amine alkaline polymer which prevents the electrolyte poisoning and allows the cell to be recharged. Two cells were built and tested which showed an open circuit potential of 1V and a maximum current density of 0.2 mA/cm^2. The measured current density is not high, but the cells were recharged three times with no degradation in performance. Future changes in the design have already been identified to increase current density including improving cathode wetproofing, improving electrode conductivity and improving the membrane electrode bond to reduce interfacial resistance.

Actual Accomplishments vs. Original Goals/Objectives

Draper originally proposed the following three projects for this subaward:

1. separating CO_2 from fossil fuel power plant flue gas mixtures using clathrate hydrates,
2. developing a catalytic reactor for reconverting CO_2 into more benign/useful chemicals such as methane,
3. continuing a collaborative Brown-Draper development of a direct carbon fuel cell.

The first project was modified to look at the potential use of clathrate hydrates for energy storage and other forms of utility-scale energy storage. Before this program was awarded, the Brown and Draper PI's for the second project received a separate DOE award, so it was replaced with a project to develop a rechargeable zinc air battery.

Technology Transfer Activities

BROWN-DRAPER ENERGY COLLABORATION

This subaward fostered a three-year old collaboration between Brown University and Draper centered on energy research and development. The collaborative relationship is based on the premise that a university is more focused on fundamental research while independent R&D labs concentrate on developing the fundamental research into practical hardware/software. Each project reported here provided opportunities for individual Draper staff and Brown faculty to interact and work together; these personal interactions are the backbone of the Brown-Draper energy collaboration.

The energy storage project provided an opportunity for Brown and Draper to build on a previous joint proposal to use clathrates as a substitute for amines in CO_2 separation from flue gas streams. It also provides new funding opportunities for Brown and Draper in the smart grid area.

The DCFC project was a very collaborative project between Brown University and Draper as both organizations were actively working on critical pieces on making a DCFC practical. The DOE award also supported the Brown PI and his graduate student who were working on the DCFC with the Draper personnel. The work accomplished in this report is being continued in the next fiscal year by both Brown and Draper.

The Zn-air battery project was primarily done by Draper but was the subject of a joint proposal to DARPA that included three faculty from Brown University.

PATENT APPLICATIONS

Provisional patent application in August 2011: "Methods for Direct Carbon Fuel Cell Operation with a Circulating Electrolyte Slurry".
The Zn-air rechargeable battery is currently under review by Draper's patent committee.

Project Summary - Energy Storage

ORIGINAL HYPOTHESIS

The need for energy storage is rising as more renewables are incorporated into the grid. Because the availability of renewables is random, GW-hr scale storage is required to satisfy end use during periods when renewables are unavailable. In addition, power companies today can use energy storage to shift daytime loads to nighttime when power production may be cheaper. The following figure shows a nominal power plant output at 1500 MW (green line) versus a typical demand load (red line). When the red line is greater than the green line, energy needs to be provided from storage (blue line) or extra generating capacity that may cost more to operate is needed to meet demand. Conversely, when the red line is below the green line, then energy can be stored. Integrating the area under the red line when it exceeds the green line is an estimate of the energy storage needed at a single power plant, roughly 10 hours multiplied by 500MW = 5 GW-hr.

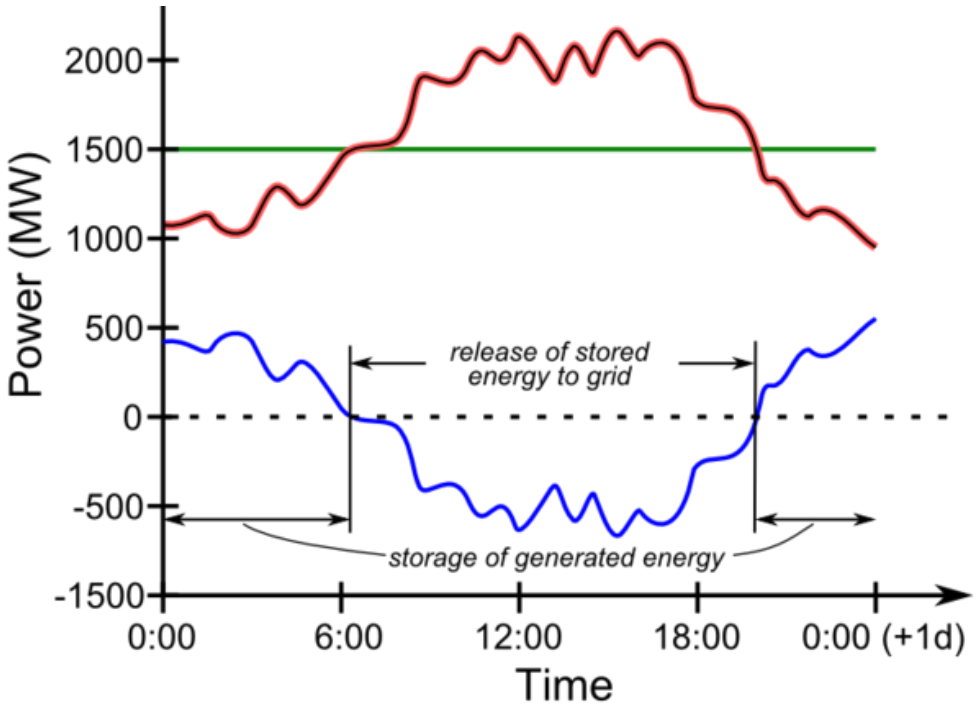

Figure 1 Energy Storage Need. Nominal power plant output (green). Power demand (red). Energy storage (blue)

Conventional energy storage technologies range from electrochemical batteries to ultracapacitors to fly wheels, but all are burdened by high costs and scalability to the GW-hr size. During various brainstorming sessions at Brown University and Draper, three concepts were proposed for low cost GW-hr energy storage:

1. pond-size galvanic cells,
2. leveraging carbon capture sequestration equipment, and
3. clathrate hydrate compression.

POND-SIZE GALVANIC CELL

Approach

Two volumes for a cooling pond were evaluated 0.05 km^3 for the Mount Storm cooling pond in West Virginia and 0.01 km^3 for a generic pond that is 1 square km by 10m deep. It was assumed that the ponds were divided in half to form a CuZn galvanic cell. The CuZn chemistry was chosen as a baseline; other chemistries are possible and perhaps more desirable. With a concentration of 0.5 mol/L (M) of salts, the Mount Storm cooling pond could store 740 GW-hr while the generic cooling pond could store 8.8 GW-hr with only 0.03M salt concentration.

Figure 2 Typical Cooling Pond

Problems Encountered

No consideration was given to the practical issues of converting a cooling pond into a galvanic cell such as implementing a porous barrier in the middle of the cooling pond to separate the Cu electrolyte from the Zn electrolyte. The ground surrounding the pond may also end up short circuiting the cell. There is no investigation into how to practically implement the electrodes. In addition, there was no consideration given to public safety or the environment.

Conclusions

The use of a cooling pond or similar size body of water as a galvanic cell shows promise. The most compelling case was the generic cooling pond which had a relatively low concentration of salts at 0.03 Molarity which was right at the GW-hr target. However, much more effort is required to evaluate safety, technical feasibility, and overcoming public perception.

HYBRID CARBON CAPTURE/ENERGY STORAGE

Approach

Carbon capture sequestration (CCS) systems currently under consideration will separate the CO_2 from the flue gas and pressurize it to 15 MPa for sequestration. If the power plant is operating at part load, then some or all of the CCS compressors may be available for compressing air for energy storage which is an accepted energy storage technology.

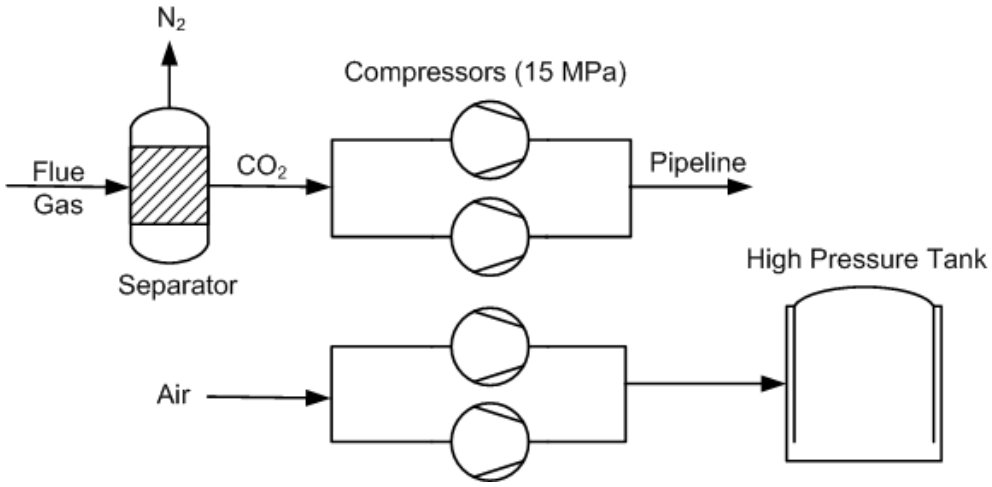

Figure 3 Schematic showing CO_2 compressors being diverted to energy storage during part load operation.

An initial estimate of equipment sizing was as follows:

- compressors: 5 x 14.4 MW
- turbines: 5 x 7 MW
- heat exchanger: 5 x 250 m^2
- tank: 1 x 9500 m^3 (for > 15MPa pressures).

The following capital cost estimates were made:

- compressors: $49 million
- turbines: $1.6 million
- heat exchanger: $0.2 million
- 15 MPa storage: $4 million.

If CCS equipment was already installed at a power plant, the capital cost of adding energy storage would only be $5.7 million. Unfortunately without CCS equipment available, the capital equipment cost would be $54 million, and almost all power plants in the U.S. do not have CCS.

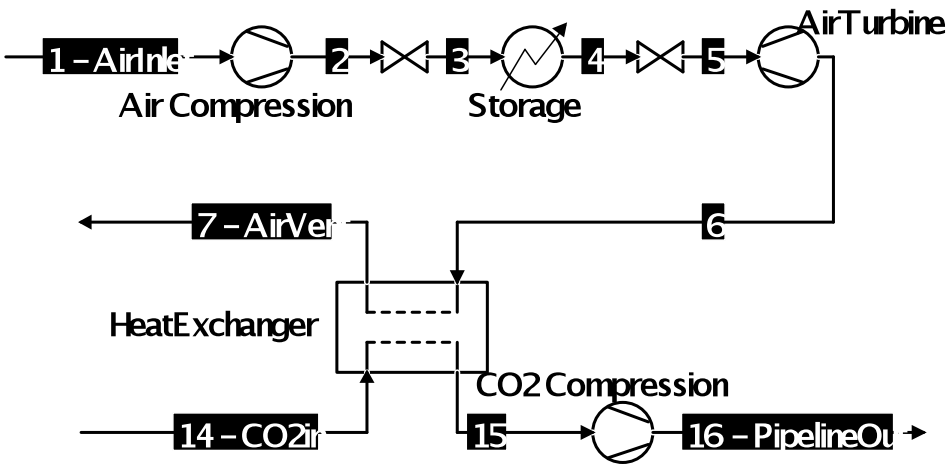

Figure 4 Schematic of Energy Storage Concept

A schematic of the proposed energy storage concept combined with CCS is shown in Figure 4. Note that the depressurized air exiting the air turbine absorbs heat from the CO_2 stream before the CO_2 is compressed to 15 MPa for sequestration. For a hypothetical 500 MWe power plant, this concept could provide 90 MW-hr of compressed air (real) energy storage as shown in the next figure. Additional energy savings (virtual) would be possible because the CO_2 compressor uses less energy with the cooling from the heat exchanger.

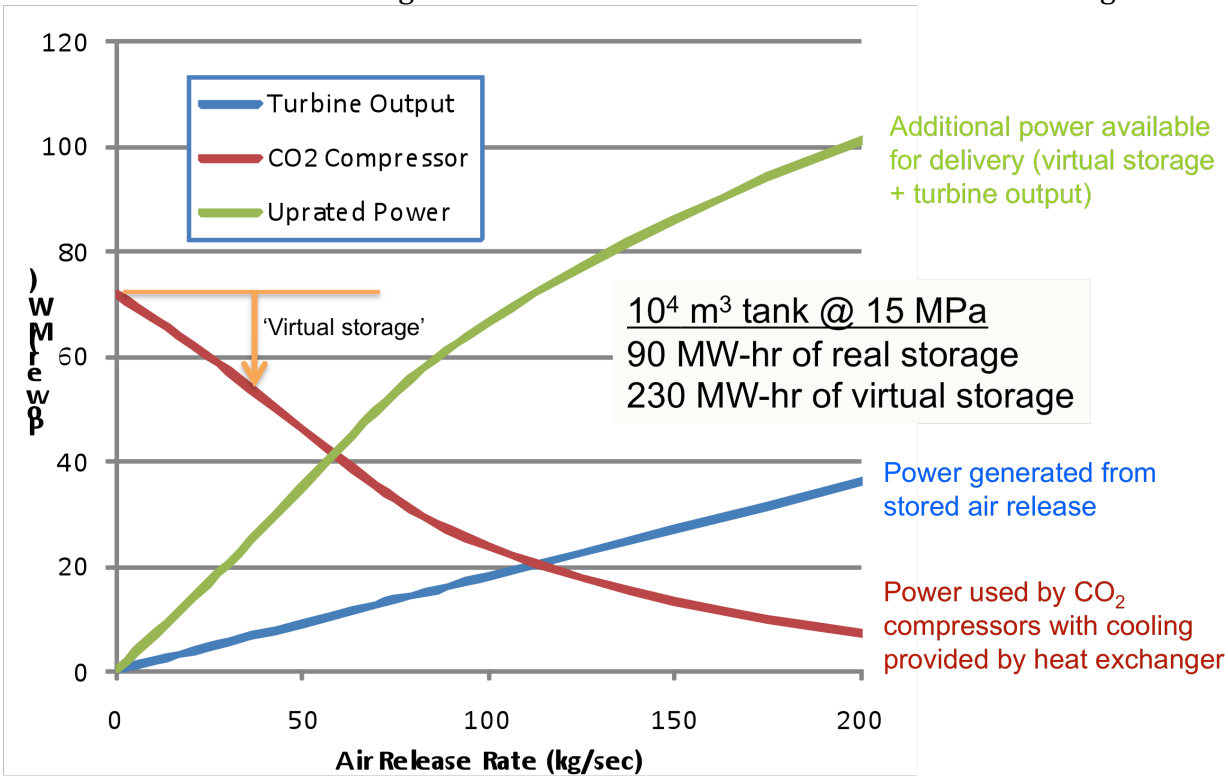

Figure 5 Process Model Results

With these results, a four year return on investment was projected when CCS equipment is repurposed for compression assuming $150/MW-hr at peak demand.

Problems Encountered

The biggest problem is the concept is economically unattractive without CCS equipment already installed, and CCS equipment adoption is almost non-existent.

Conclusion

Assuming widespread adoption of CCS as currently envisioned occurs in the future, this concept will be a useful way to implement energy storage simultaneously.

CLATHRATE COMPRESSION

Approach

Because liquids are much less energetically and financially expensive to pump relative to compressing a gas, this concept used clathrate hydrates to convert a gas such as air to a liquid to enable low energy/cost pumping to desired pressures. Like the previous concept, the energy is stored as a compressed gas.

Assuming the clathrate hydrates have similar properties to water, the energy to pressurize 120 kg/second of CO2 gas is roughly an order of magnitude higher (67 MW versus 6.18 MW) than pumping 300 kg/second of water to the same pressure as shown in the following tables.

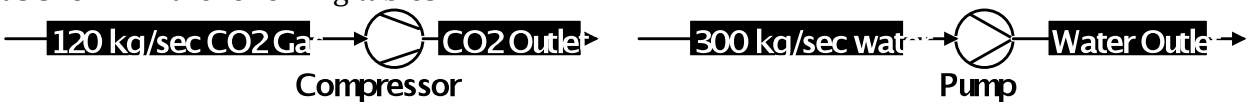

Compressor		
Parameter	Value	Unit
Isentropic efficiency	0.85	
Pressure	15	MPa
Energy demand	67.321	MW

Pump		
Parameter	Value	Unit
Adiabatic efficiency	0.85	
Pressure	15	MPa
Energy demand	6.17734	MW

Stream	120 kg/sec CO2 Gas	300 kg/sec water	CO2 Outlet	Water Outlet	Unit
Pressure	0.1	0.1	15	15	MPa
Temperature	20	20	568.207	21.4148	°C
Flow rate	120	300	120	300	kg / s
Enthalpy	−363135	−2.55984e+006	557377	−2.53925e+006	J / kg
Entropy	−13.9436	−6910.76	90.3465	−6900.23	J / kg °C
Volume	0.550638	0.00117466	0.0109008	0.00117371	m^3 / kg

The following process cycle was proposed and analyzed:

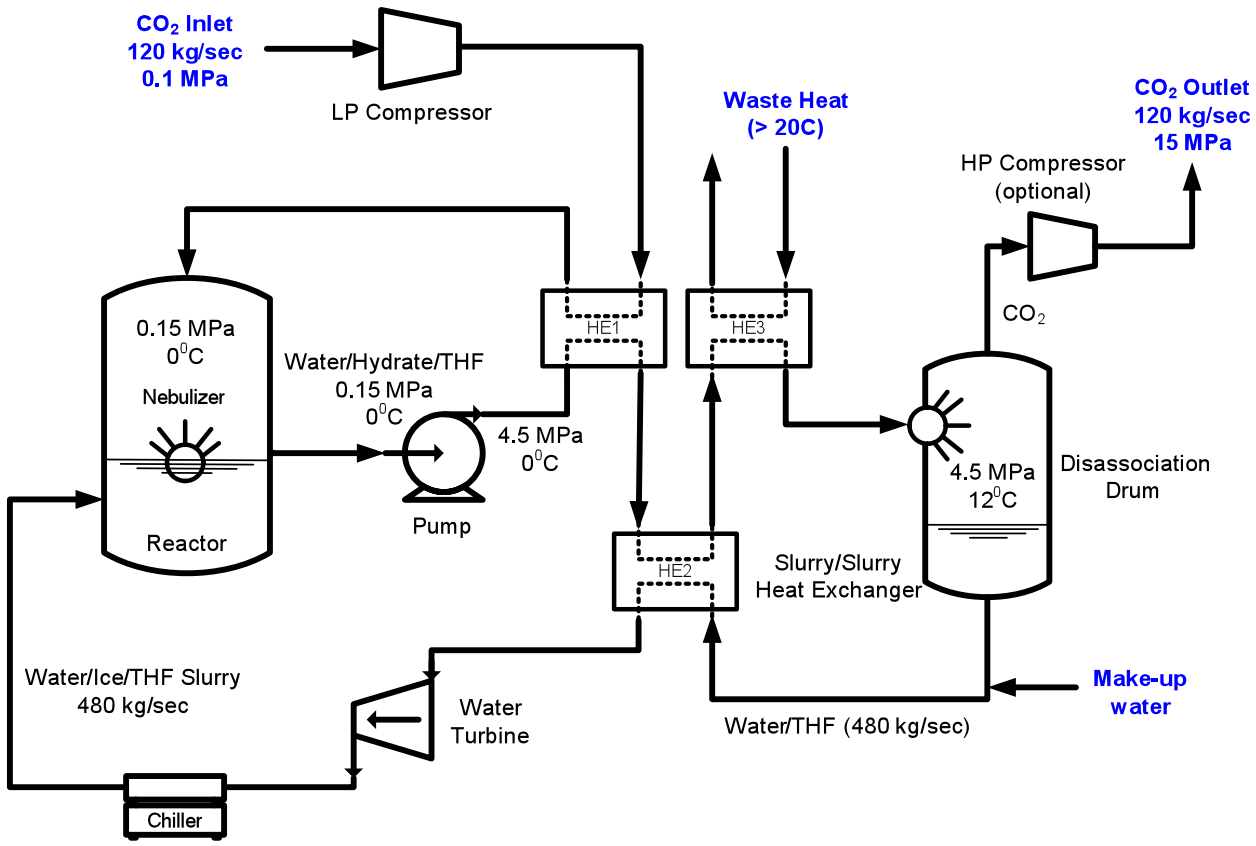

Figure 6 Clathrate Compressor Cycle

The CO_2 gas is trapped by the clathrate hydrates (with tetrahydrofuran, THF, as a clathrate promoter) in the reactor at left. Then the CO_2 clathrate slurry is pumped to 4.5 MPa. In the dissociation drum at right, the CO_2 is released from the clathrate at 4.5 MPa and further compressed to the desired 15 MPa. The water/hydrate is run in a closed loop.

Problems Encountered and Conclusion

Unfortunately, a chiller is required to bring the water temperature from 12ºC to 0ºC which also includes the heat of formation. The waste heat introduced at HE3 causes a net addition of heat but is required to release the gas from the clathrate. Ideally, the water coming out of the water turbine could be used as the waste heat source at HE3, but the two streams are at nearly identical temperatures.

The following table summarizes the equipment cost and operating cost of the clathrate compression scheme with traditional compressors. The clathrate compressor with the chiller is more expensive to operate than the traditional compressor. If the chiller is eliminated then the clathrate compressor is very competitive with traditional compressors.

	Traditional Compression	Clathrate Compressor	Clathrate Compressor (w/o chiller)
Equipment cost	$40.1M	$37.5M	$16.5M
Operating Cost	$27.3M/yr	$48M/yr	$4.6M/yr

Project Summary - DCFC

ORIGINAL HYPOTHESES

Any proposed system design will require a method to clean the electrolyte after some duration of operation. This includes removing solid inorganic particles (ash) and chemical impurities such as carbonate and possibly sulfur. To solve this issue, two electrolyte cleaning techniques were developed.

Over the past several years Dr. Joseph Calo from Brown University has been investigating the use of hydrodynamic DCFC cells where an inert lift gas drives circulation and flow. This is directly analogous to a fluidized bed. It is anticipated that this approach will solve two critical DCFC issues; fuel transport and anode charring. This system concept development effort began using this hydrodynamic DCFC as a baseline approach.

The core of this project was the generation of a thermodynamic model to fully evaluate performance under various conditions. Due to the complexity of the system, it was decided to only model the vaporization cleaning method. Overall, this system is easier to model and more conservative regarding parasitic energy losses due to the high heat of vaporization for sodium hydroxide.

This thermodynamic model is intended predict system level efficiency performance of a DCFC. Many studies have presented the efficiency of a DCFC cell, but never an entire system with fuel and electrolyte processing. In addition, the model gives key insight into performance sensitivities to unknown parameters, such as carbonate formation and the Boudouard reaction.

APPROACH

System Level Concepts

Four system level concepts were generated. These designs consisted of schematic layouts for the entire cell and critical sub-systems (ash removal, pyrolysis, etc). Prior-art was used to generate approximations on, efficiency, flow rates, and cost for the various subsystems, and consequently the systems as a whole.

For each system, design features were compared against concept selection criteria. These were used to down-select an optimal system and precede to subsequent detailed design activities. The optimal system shown in Figure 7 hydrodynamically transported the carbon/electrolyte slurry through a tortuous path in the anode reactor. To start the process, pulverized carbon and recycled hydroxide are mixed and fed into the front end of the cell (left side). The resulting slurry is entrained and carried into the start of the labyrinth. Small lift gas ports are located at the base of each vertical column pair. Steam flowing from these ports induces vertical flow, which transports slurry to the next column. The last column pair overflows into a drain port, which is fed into the cleaning system.

Overall mass transport through the cell is controlled by the quantity of carbon and sodium hydroxide fed into the front of the cell. The mixing and concentration gradients, however, are controlled by steam flow through the lift gas ports. It is hoped that optimizing these parameters and the cell geometry will cause complete carbon reaction before the slurry is expended from the end of the cell.

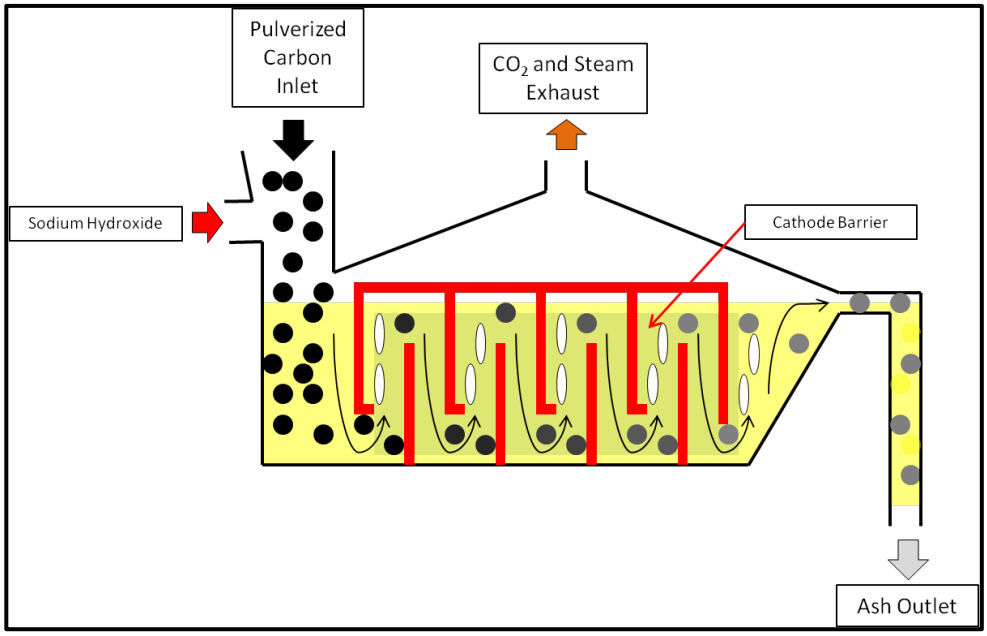

Figure 7: Optimal Concept – Hydrodynamic Labyrinth

This concept satisfied many of the desired design criteria. The slurry is hydrodynamically mixed and passed through the cell. This should prevent clogging/charring while simultaneously abrading carbon particles to remove ash layers. There is also potential to add vanes, or fins, within the column pairs to increase anode surface area and reduce internal cell resistance. The overflow feature means the slurry height in the reactor is self-regulating.

The primary drawback is this concept is that it may require a long labyrinth to ensure complete carbon consumption. This will involve a large cell with increased fabrication cost. It might also reduce efficiency from the large volume of lift gas

consumed to transport and mix the slurry. Unfortunately, the length of the labyrinth and required flow rate of lift gas required experimental validation.

CAD Renderings of down selected Concepts

3D models were generated for the optimal system design using SolidWorks. Sizing of the rendered cell was decided during the system modeling activity. Preliminary CAD renderings of the above system concept were generated to assess manufacturability and scale of the proposed 67 kW system. Additional cell level detail was added to illustrate flow field geometry and construction methods.

Figure 8 below details a single cell assembly through multiple views, in both assembled and exploded configurations. Both anode and cathode flow field plates are intended to be solid metal coated with a specialized ceramic layer, such as zirconium nitride. The center layer within the cell is a thin layer of highly porous zirconium cloth. This forms a corrosion resistant ionic conduction layer that electrically insulates the anode and cathode. Finally, a thin, porous, metal mesh separates the anode and cathode flow field plates on either side of the central zirconium cloth. Each mesh layer is welded or sintered to its respective flow field plate.

Multiple cells are clamped together in series to form a cell stack. Compression forces around the perimeter of the cell plate locally crush the zirconium membrane creating a liquid seal. This serves to keep the mold hydroxide contained in the anode compartment. Additional ceramic cement or crushable features may be required if this process is prone to leaks.

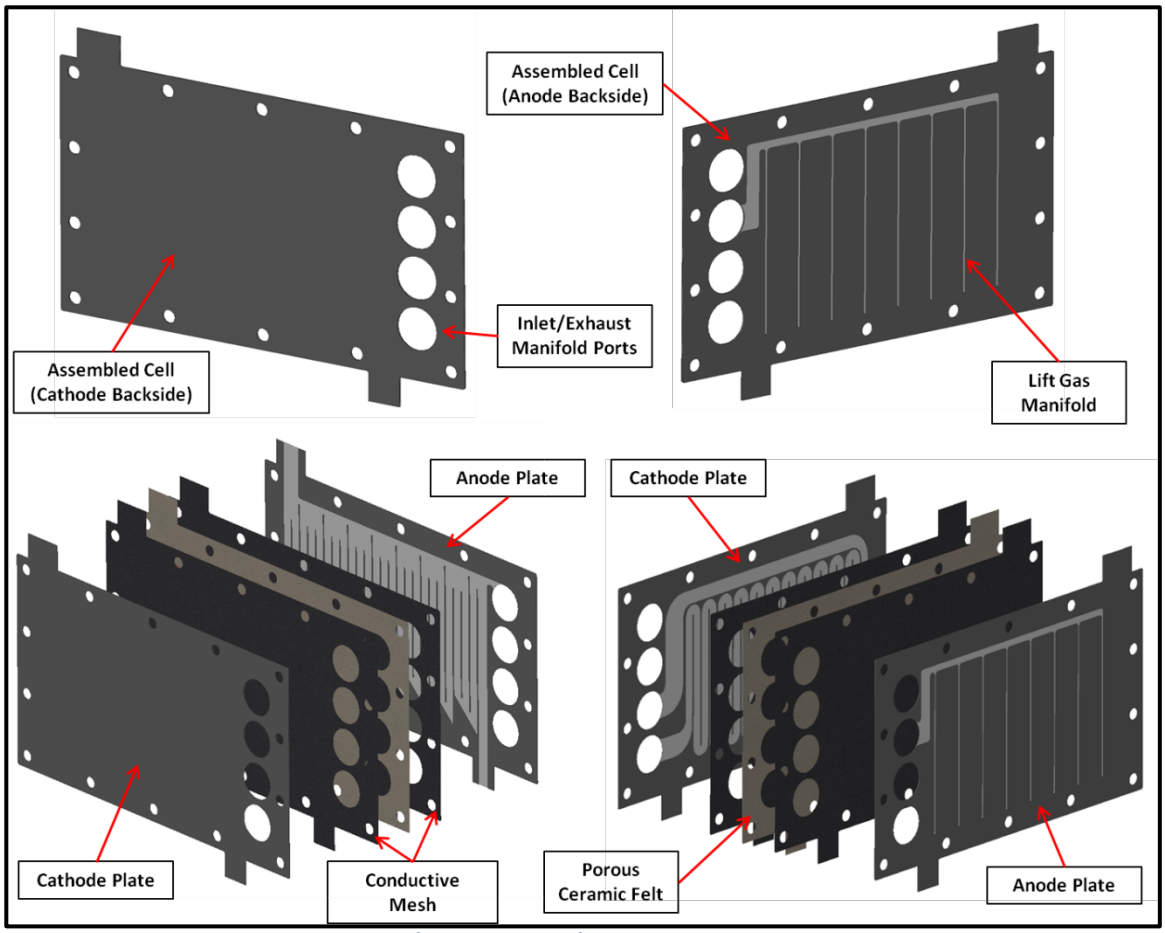

Figure 8: CAD Model for a Single Cell (67 kW System)

Figure 9 below shows notional detail of the anode and cathode flow field geometries. The cathode (right side) features a serpentine flow field transporting fresh air and steam to one side of the cell. The anode (left side) contains red portions that represent the carbon and sodium hydroxide slurry. The air head space above this liquid in the anode chamber will be a combination of steam, carbon dioxide, in trace amounts of carbon monoxide. Lift gas steam ports are small holes located at the bottom of each tetrahedral column. The supply manifold for lift gas is machined in the back side of the anode plate. This can be viewed in the upper right panel of Figure 8. These illustrations are intended to demonstrate the general flow of materials through each cell compartment. They also provide an approximation for the volume of material required to produce a cell of the size. For reference, these plates measure 4 feet in length by 2.5 feet in height. The total stack thickness is slightly less than 3/8 inch.

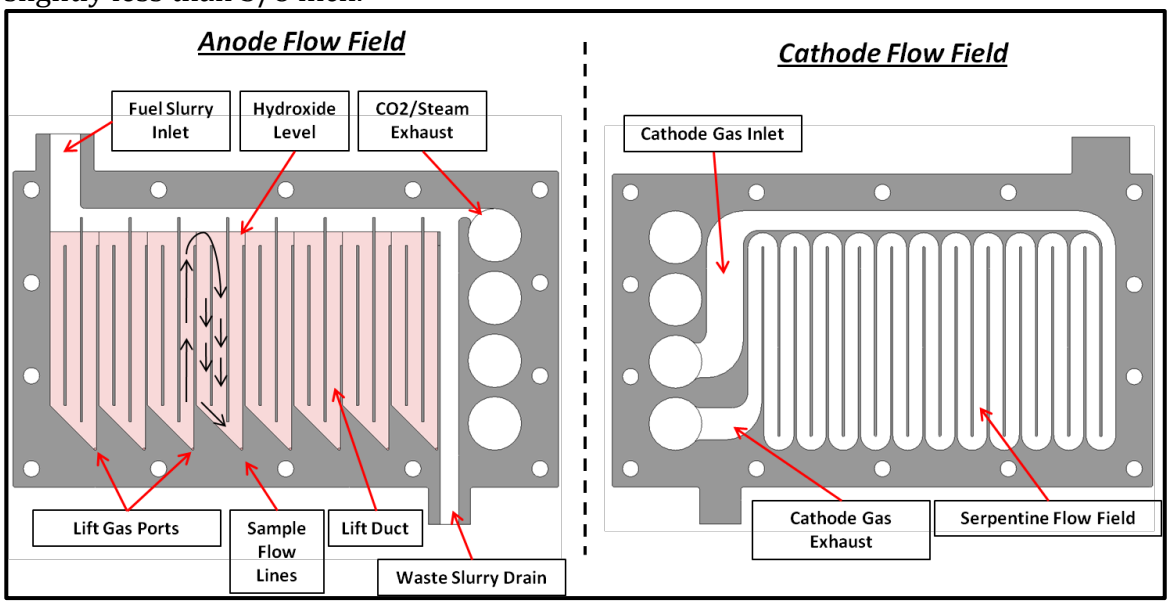

Figure 9: CAD Model of Anode and Cathode Plates

Figure 10 and Figure 11 show one possible embodiment of this direct carbon fuel cell system. The 300 cell stack is located in the center of system. As indicated by the rendering, this stack is quite large extending almost 9 feet. The figure also shows sporting equipment such as the vaporizer, fuel pyrolyzer, steam generation system, and fuel pulverizer. Figure 11 shows additional detail and component annotations.

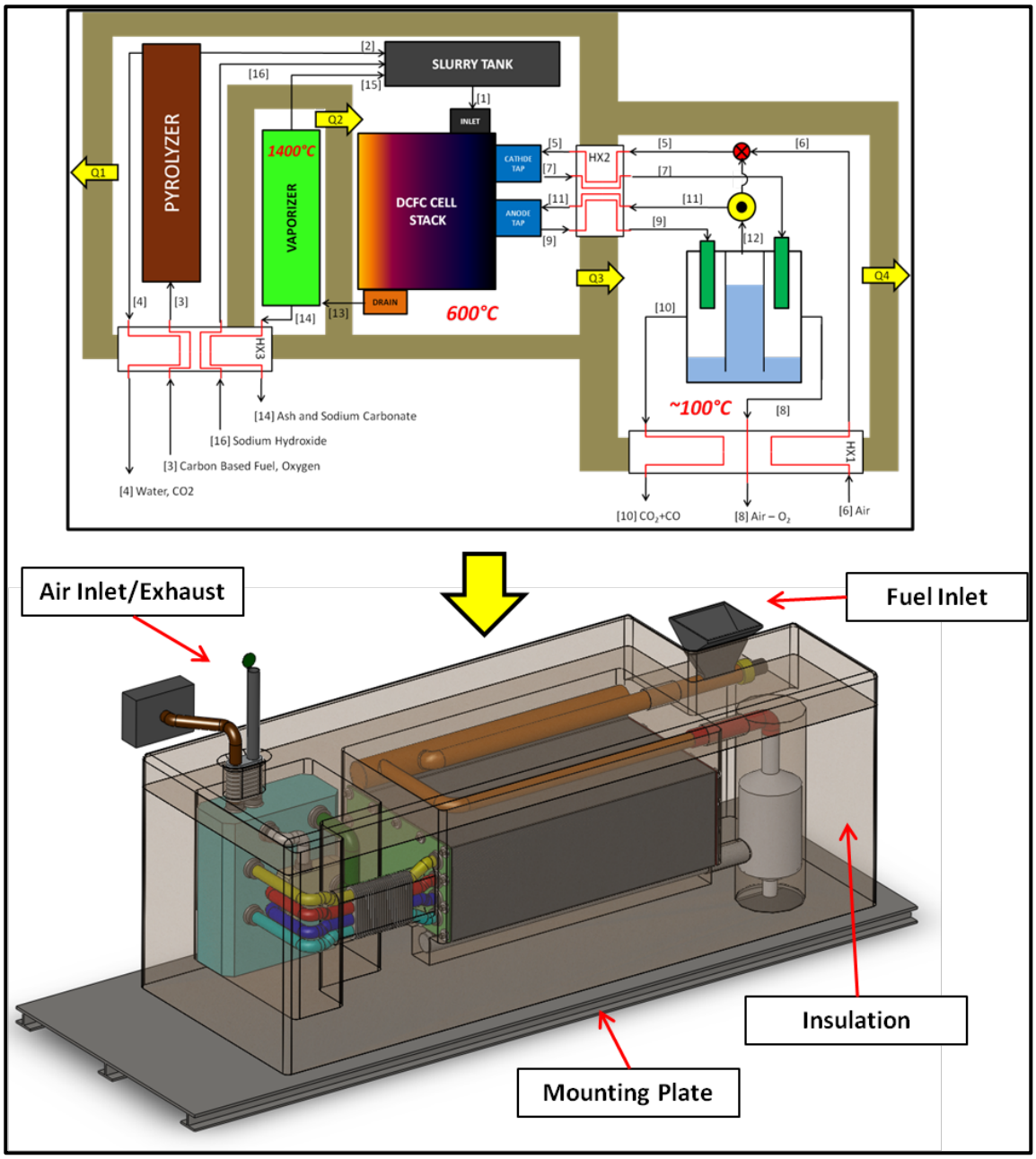

Figure 10: Envisioned 67 kW DCFC System

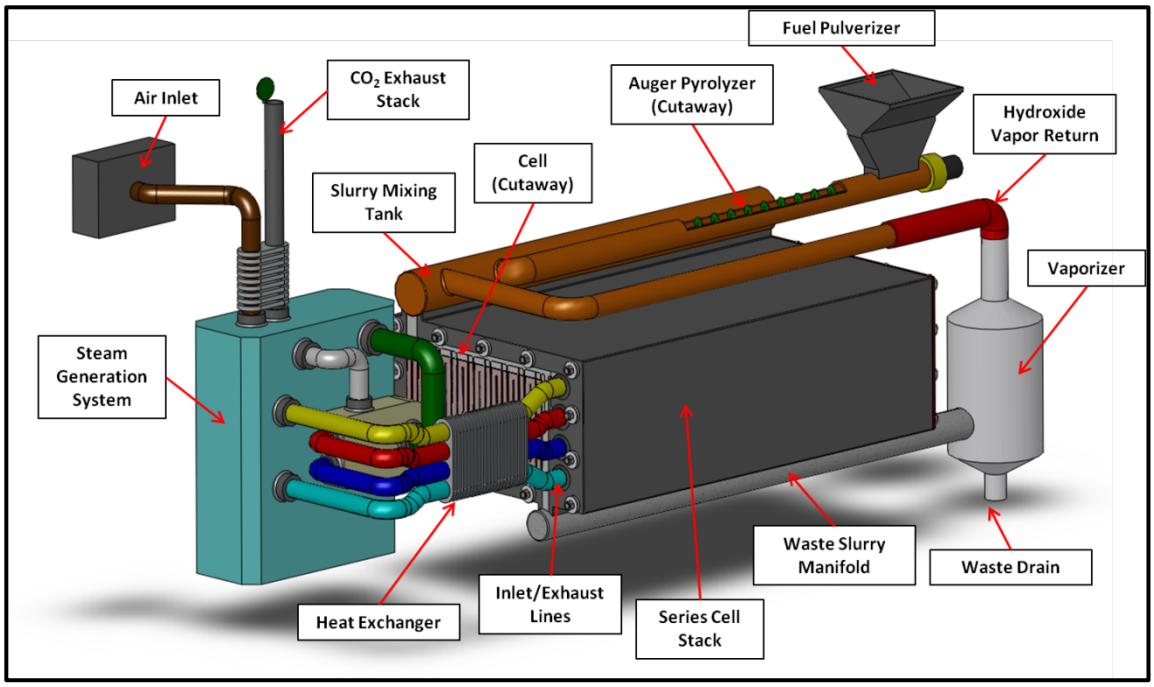

Figure 11: 67 kW System Detail

Figure 12 depicts this DCFC system located on a standard tractor-trailer bed. In this layout, the additional space on a trailer can be used to hold and process organic fuels such as wood or switch grass.

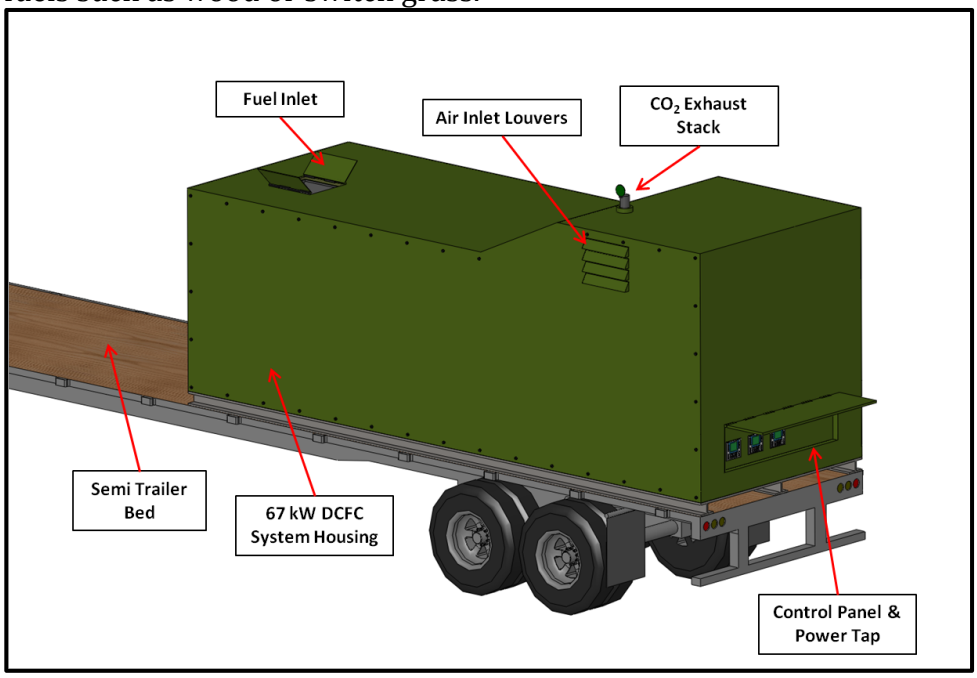

Figure 12: Portable 67 kW DCFC System

System Modeling

There was an operational overview of system to accompany the solid model design. Flow diagrams were used to illustrate material and energy flow and the resulting steady state operational performance characteristics.

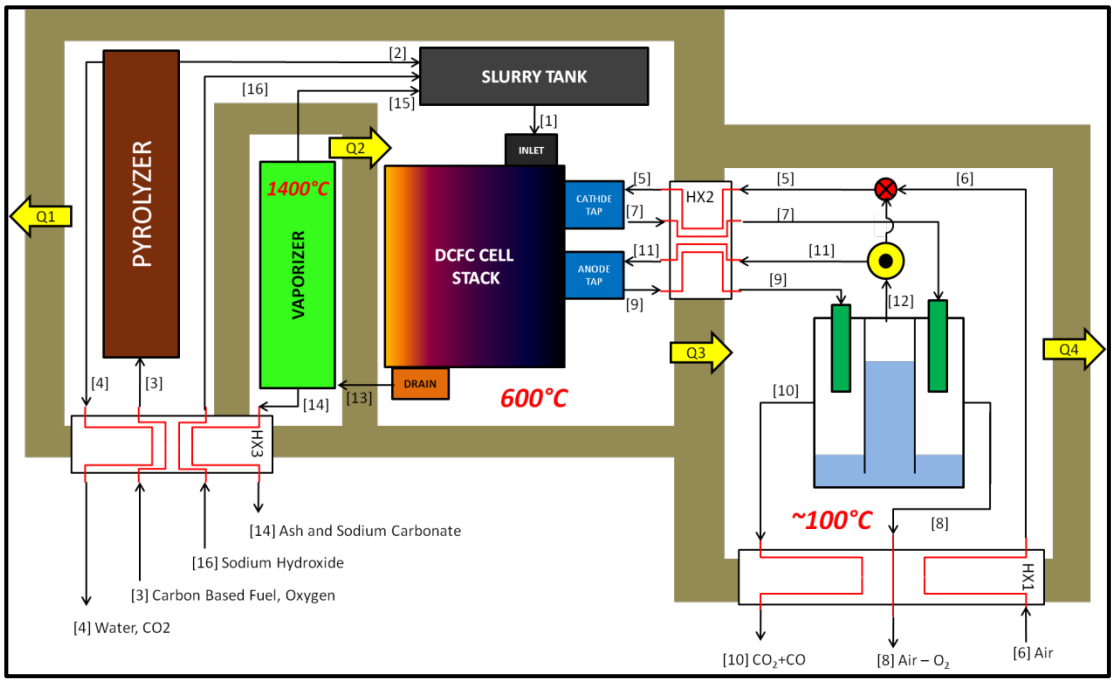

Figure 13 System Schematic

Table 1 below shows a qualitative summary the model shown above. The table is split into three columns, which represent key system parameters. These include maximum achievable efficiency, maximum total power output, and the variable cost to produce a kWh of electricity.

Efficiency is most affected by inlet slurry density and lift gas flow rate. Internal cell resistance, carbonate production, and the Boudouard reaction are second-order effects. The maximum power output is most affected by cell resistance, but inlet slurry density and lift gas flow also have considerable impacts. Carbonate production actually increases maximum power output, but there is a large negative effect on variable cost per kWh. Cell resistance and lift gas flow rate also have noticeable impacts on variable cost.

Table 1: Sensitivity Analysis Results Summary

Parameter	Effect on Max Efficiency	Effect on Max Power	Effect on Variable Cost
Cell Resistance	Moderate	Very High	High
Slurry Density	Very High	Very High	Very High
Air Flow	Very Low	Very Low	Very Low
Steam Flow	Negligible	Negligible	Negligible
Lift Gas Flow	High	High	High
Boudouard Reaction	Moderate	Low	Low
Carbonate Production	Moderate	Moderate	Very High
1 - Negligible			
2 -Very Low			
3 - Low			
4 - Moderate			
5 - High			
6 - Very High			

The results of this sensitivity analysis will certainly shape future design considerations. Initially, the vaporizer concept was preferred; however, the study reveals that a circulating cell may be more effective because of reduced lift gas rates. The study also revealed what experiments will be critical in predicting system performance. Most importantly, carbonate production needs to be well understood. Even moderate levels of carbonate production increase variable cost beyond current coal-fired electric power generation.

As expected, high lift gas flow rates have negative effects on all system parameters. Future computational fluid modeling the cell designs should place high emphasis on low lift gas consumption. This modeling effort should also increase slurry density as high as possible, although this will likely conflict with lift gas flow.

Many of the parameters in this model are related. For example, increasing cell temperature will affect carbonate formation, cell resistance, and the Boudouard to reaction ratio. Future modifications to this model should include these relationships using supporting experimental results.

Materials Testing

Another aspect of this project was investigating materials for electrode construction. The electrode material needs to be highly corrosion resistant, while maintaining electrical conductivity on the surface. These are conflicting requirements, which makes this especially challenging. Literature suggests pure nickel performs moderately in molten sodium hydroxide, but still suffers from oxidizing deterioration and sulfur contamination. This effort looked at a evaluating other metals and alloys noted for their superior corrosion resistance at high temperature compared to nickel.

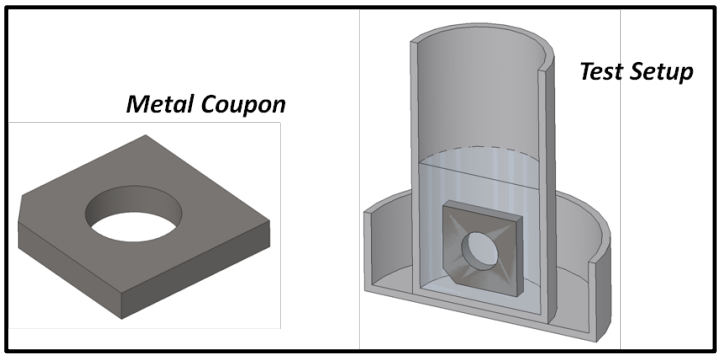

Figure 14: Illustration of Test Coupon and Crucible

Five preliminary metals and alloys were selected. These materials included Stainless Steel 316L, Titanium grade 4, Hastelloy X, Alloy 600 (Inconel 600), and Nickel 200/201. The Nickel samples will be used as a baseline to compare against current work. Besides titanium, these metals were selected for their high levels of chromium.

Figure 14 above shows an illustration of the test apparatus used to evaluate corrosion resistance in sodium hydroxide 600°C. High form Alumina crucibles were used to contain the molten sodium hydroxide and metal coupons. Figure 15 below shows additional detail and texturing of the metal coupons. The backside of each coupon was given a textured surface using a fly cutter. This was intended to give additional insight into corrosion performance with each of the imaging techniques. Two coupons were machined for each of the five metals. In addition, a thin nickel 200 mesh was tested to measure the effect of changing surface area to volume ratios.

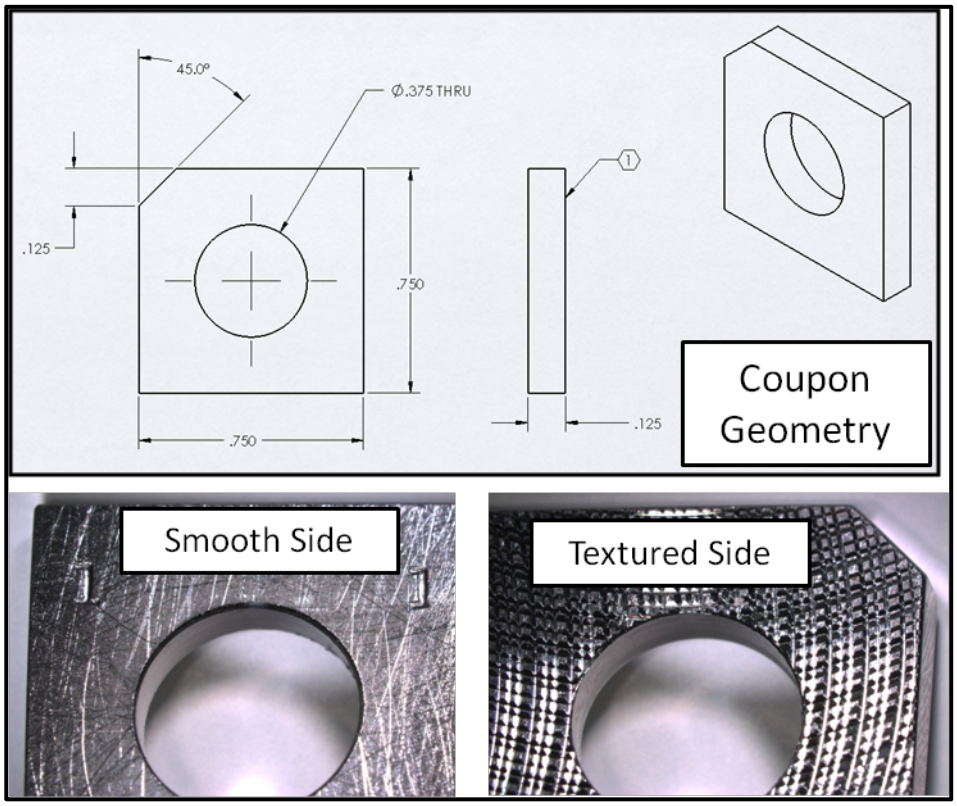

Figure 15: Test Coupon Geometry and Texture Detail

PROBLEMS ENCOUNTERED

The optimal concept had an initial risk associated with the hydrodynamic fuel transport through the anode reactor. It was unknown how effectively the sequential lift gas columns would transport solid material through the cell. To address this risk, a small scale cold flow prototype was developed, which is shown below in Figure 16. It should be noted that this prototype only represents the anode compartment of the cell.

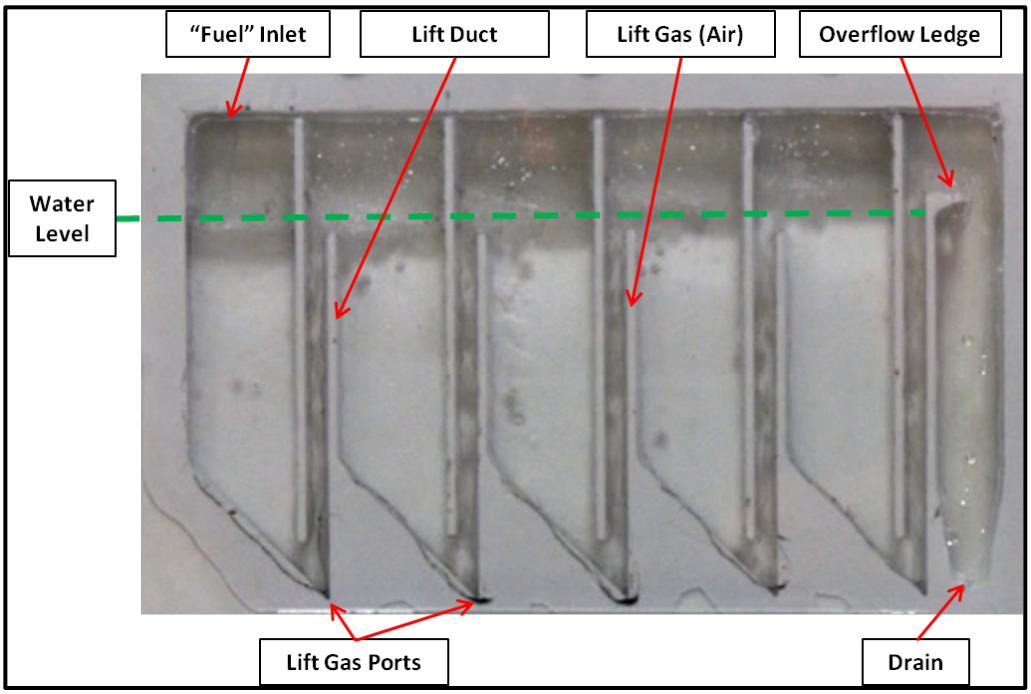

Figure 16 Cold Flow Prototype Overview

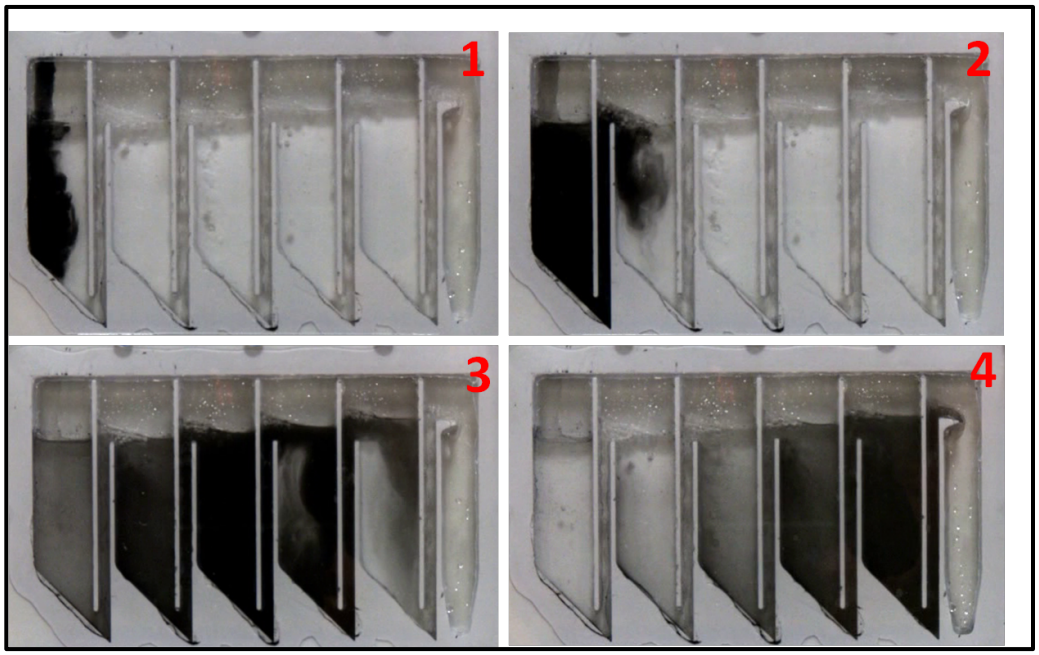

Figure 17 Cold Flow Prototype in Operation

Figure 17 shows images from this demonstration cell in operation. To highlight solid transport, a small volume of fly ash slurry was introduced at the cell inlet at the upper left corner. This was accomplished by switching the circulation pump inlet to a small container holding the dense fly ash slurry. Once extracted, the pump inlet was re-connected to the cell drain port.

Frame 1 in the upper right panel of Figure 17**Error! Reference source not found.** shows the fly ash slurry entering the first column pair. Frame 2 shows the slurry being driven up the first lift duct and into the second column pair. Frames 3 and 4 demonstrate the movement of solids through the cell towards the drain port. Frames 1, 2, 3, and 4 occur at times 0, 4, 22, and 42 seconds, respectively.

This demonstration proves this concept's ability to transport solid material through a tortuous path on the anode chamber. As Frame 4 indicates, this prototype was also effective at preventing back mixing as the first column pair has been cleared of solids.

CONCLUSIONS

Under nominal conditions, the system modeled in this study can achieve a 54% HHV efficiency while generating 22 kW. Variable fuel cost at maximum efficiency is 1.9 cents per kWh, which is a 34% reduction over existing coal generated electricity. Maximum power output is 67 kW, but efficiency drops to 30%.

These performance numbers are impressive compared to combustion-based power generation. However, the physical footprint of the above system is extremely large compared to a diesel driven portable power generator capable of the same power output. Each cell is approximately 4 feet long, 2.5 feet tall, with a depth of 0.35”. A total of 300 cells were required to generate the power output listed above, which means the cell stack alone has a depth of almost 9 feet. The weight of the cell stack alone could easily exceed 20 tons. Depending on the material selected, capital cost of the electrode plates would completely offset economic feasibility of the system. Unless the internal cell resistance can be dramatically reduced over current values, this technology will be expensive and impractical.

The CAD modeling effort highlighted two key insights into the development of this technology. First, internal cell resistance will need to be reduced over currently measured values. This model used the cell voltage of 0.6 V at 100 mA/cm2. Under these conditions, the cell stack required to produce 60 kW measures 4' x 2.5' x 9'. If made from pure nickel, the anode and cathode plates alone would weigh 18 tons and cost just under $385,000 with current market prices. This results in a capital cost of $6,400 per kilowatt hour for just the electrode plates. This is over three times the capital costs for coal-fired power plants.

A second insight discovered was difficulty developing an effective inlet slurry manifold. Each cathode and anode plate in a series cell stack must be electrically insulated from each other. The electrolyte slurry is conductive; therefore there must be a liquid break between each cell. The current model does not include a manifold capable of effectively supplying fuel slurry to each cell without galvanic short-circuiting of the stack. This is further evidence to reduce internal cell resistance, which will allow for less cells and a more feasible manifold design. This suggests having more cells in parallel with a common slurry inlet bath.

In summary, pure nickel performed best in molten sodium hydroxide. Despite promising results with a solid sample, testing of an un-sintered mesh showed that even nickel will likely fail over long periods of operation in sodium hydroxide. It is

suspected that some form of conductive ceramic material will be required. Particular candidates include zirconium nitride and chromium nitride. Testing is currently underway to evaluate these compounds.
Corrosion remains a severe problem preventing the development of reliable long term operation DCFC cells.

Project Summary - Zn Air Rechargeable Battery

ORIGINAL HYPOTHESIS

As electronic devices get smaller and smaller, the energy to operate them has not changed significantly and is therefore becoming a larger portion of the device's size and weight. Energy densities have to improve in order to continue miniaturization. Zinc air chemistry is well known with an energy density of 340 whr/kg and 1050 whr/liter, far above the best lithium ion cells. While lithium air cells have a higher thermodynamic potential (energy density ~1,700 whr/kg), the safety implications make zinc a much more attractive metal. Zinc is also plentiful, cheap and a local resource. It can also be shipped via standard methods and disposal is akin to any alkaline battery.
The downside of current zinc air batteries is that most of them are primary cells. While there are several key companies developing rechargeable versions, they are plagued by problems with CO_2 poisoning or practical mechanical zinc replacement issues. In addition, they make noise due to the fan flow needed to provide air which limits their stealth applications. While soldiers have issues with all batteries that do not provide a state of charge, the zinc air is more of a challenge because it must be kept in a foil bag (no air) to limit its self discharge.
The following figure is a schematic for the rechargeable Zn air battery.

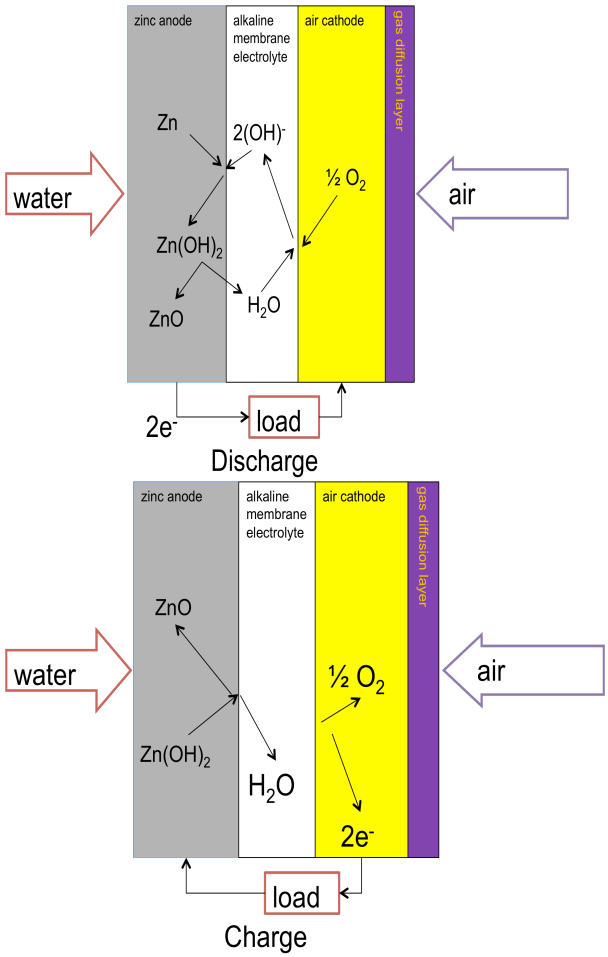

Figure 18 Rechargeable zinc air battery schematic. (Left) battery discharging; (right) battery recharging.

The zinc air concept developed here is solid state. It is based on alkaline polymer technology. There is no liquid electrolyte. The only liquid is water. The water is required to form the hydroxide ions which combine with the zinc to form zinc hydroxide and 2 electrons. If it is possible to keep the water separate from the cell until discharge is needed, then the cell remains stable and no foil bag is needed. Humidity remains a challenge. It is relatively immune to CO_2 poisoning (based on air concentrations) because it is based on a quaternary amine membrane which promotes an ion flux that counteracts CO_2 diffusion.
An initial system analysis of a Zn-air cell predicted 1.24V with a current density of 13.6 mA/cm^2.

APPROACH

The crucial issues associated with zinc-air technology are rechargability, zinc dendrite formation, CO_2 poisoning and recrystalization of the anode catalyst through multiple charge/discharge cycling. Our concept consists of a solid state quaternary amine based membrane with bifunctional cathode catalyst to enable electrical recharge.

The carbon dioxide poisoning is prevented by an anionic exchange polymer membrane using a quaternary amine functional group. Ionic mobility in such a membrane should be high, so the quaternary amines limit the mobility of the CO_2.
For the zinc electrode, particle size, distribution, electrical conductivity, porosity and corrosion rate are all vital to the performance and cycling capability of the anode. Zinc air batteries are not known for their fast response to current draw or high performance. Through a combination of high surface area and improved electrical conductivity, the performance should improve. The essence of the reaction is the interface of zinc and hydroxide within the polymer. Very thin coatings of polymer on the zinc slurry are ideal. As with fuel cells, maximizing the available sites and providing short conduction paths for the electrons and ions will facilitate better performance. The 325 mesh particulate zinc was mixed with 25-30% by weight polymer resin and pitch based carbon fibers. The fibers act to improve electrical conductivity and improve the point-to-point particle connections. The solution was cast onto a thin piece of carbon paper which adds strength to the layer. The carbon paper is 70% porous and allows water to flood the backside of the electrode. The NMP solvent in the resin was allowed to air dry for several days.
For the cathode electrode, the bifunctional catalyst (proprietary) is mixed with 25% by weight resin and is cast onto a teflonated sheet of nickel felt. The cast layer was allowed to air dry for several days. The catalyst particles were too heavy and did not form a suspension in the resin. It was, therefore, difficult to distribute the catalyst over the surface of the felt uniformly. The nickel felt was unsintered since a sintered sheet was unattainable during the period of performance. This may contribute to the overall high cell resistance. In addition, the layers were not pressed prior to building into an MEA (membrane electrode assembly). Thus, the electrical resistance of the layers may be high. These cells represent a baseline. An optimization on the recipe varying resin content and press pressure would be prudent. Thin resin layers on the particles are needed but the particles must still touch to conduct electrons through the layer (away from the membrane) and into the current collector.
Two prototype cells were assembled; each consisted of a cathode and an anode which are then lightly pressed together with a membrane in between to form a membrane electrode assembly (MEA). The critical components of the three parts are listed in the table below.

Table 2 MEA component matrix

Membrane	**Cathode**	**Anode**
Fumapem FAA-3 membrane	Gold plated nickel catalyst	zinc particles
	Fumion FAA-3 resin	pitch based carbon paper chopped up
	teflonated nickel felt gas diffusion layer	Fumion FAA-3 resin

Photographs of the cathode, anode, and MEA are shown in the following three figures.

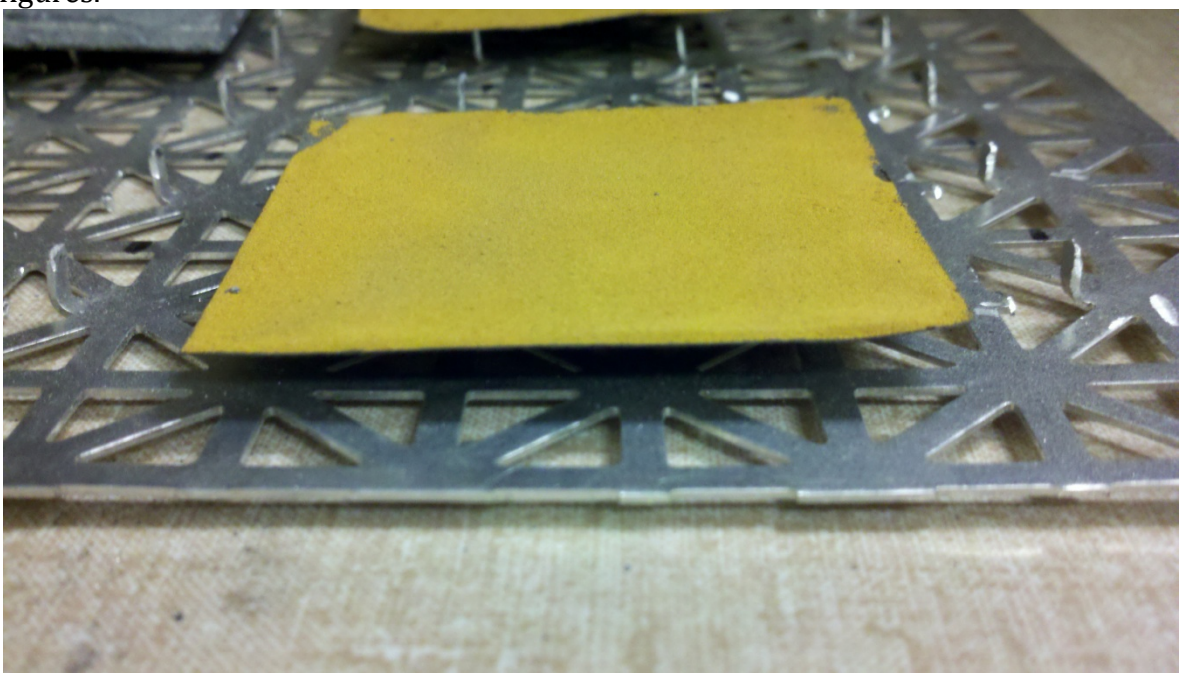

Figure 19 Cathode (yellow sheet 2.5" by 2.5") resting on drying rack.

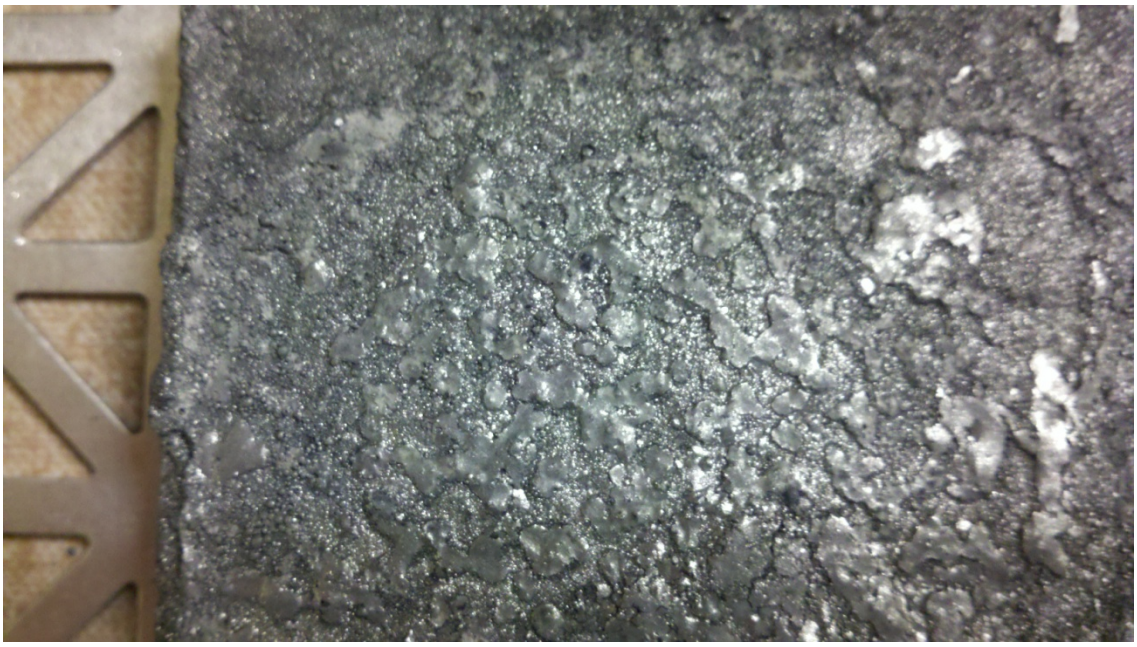

Figure 20 Anode.

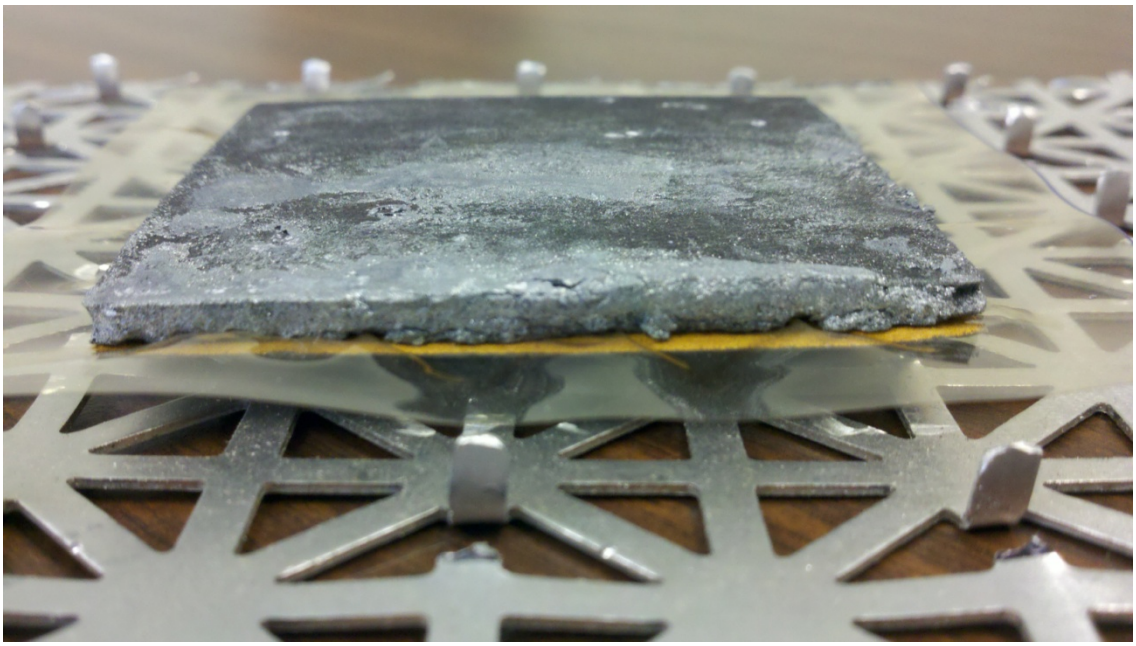

Figure 21 MEA. Membrane is translucent sheet between cathode(yellow) and anode (black)

A good bond is established between the membrane and electrodes on initial contact which could be related to residual resin that is still drying in the electrode layers. After the MEA was assembled, it was converted from the chloride form to the hydroxide form by soaking it in a weak 0.5 molar NaOH solution for 24 hrs then rinsing in deionized water. The amines in the membrane quickly turn brown on exposure to NaOH. The membrane expansion during conversion and rinse caused the electrodes to delaminate almost completely from the membrane. The MEA was placed in a fixture that flowed air over the cathode and water over the anode.

It should be noted that the nickel felt was teflonated using typical wetproofing methods employed in fuel cell air cathodes. The wetproofing keeps the pores in the nickel felt from getting clogged with water. If that occurs, the oxygen must diffuse through the water layer to get to the catalyst. The wetproof layer showed good hydrophobicity directly after treatment (Figure 22 left photo). However, after chemical conversion and rinse, the wetproofing appears to be defeated (Figure 22 right photo).

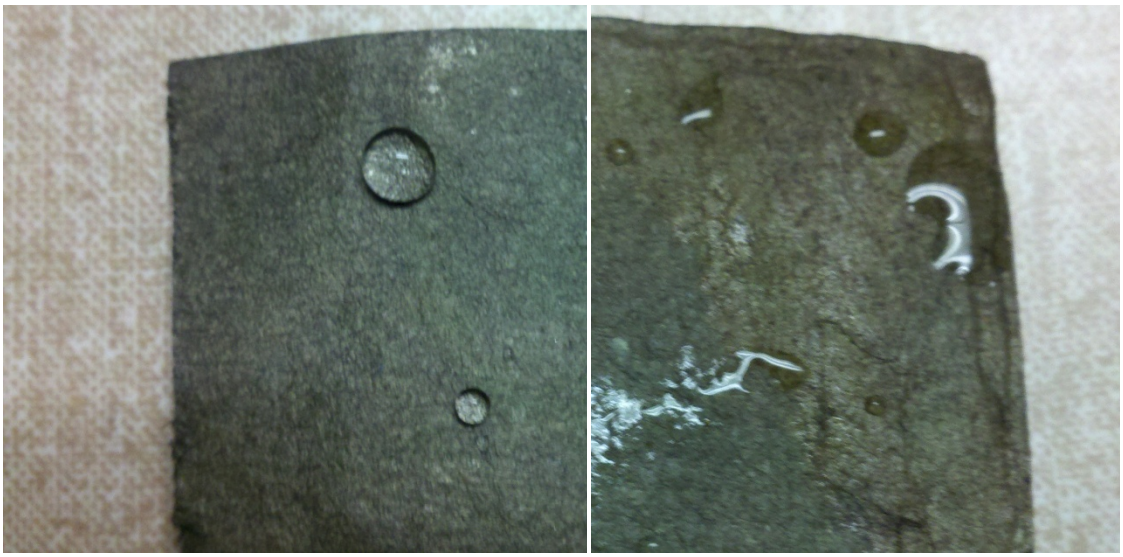

Figure 22 Gas diffusion layer wetproofing. L: wetproofing working before conversion. R: wetproofing failing after conversion.

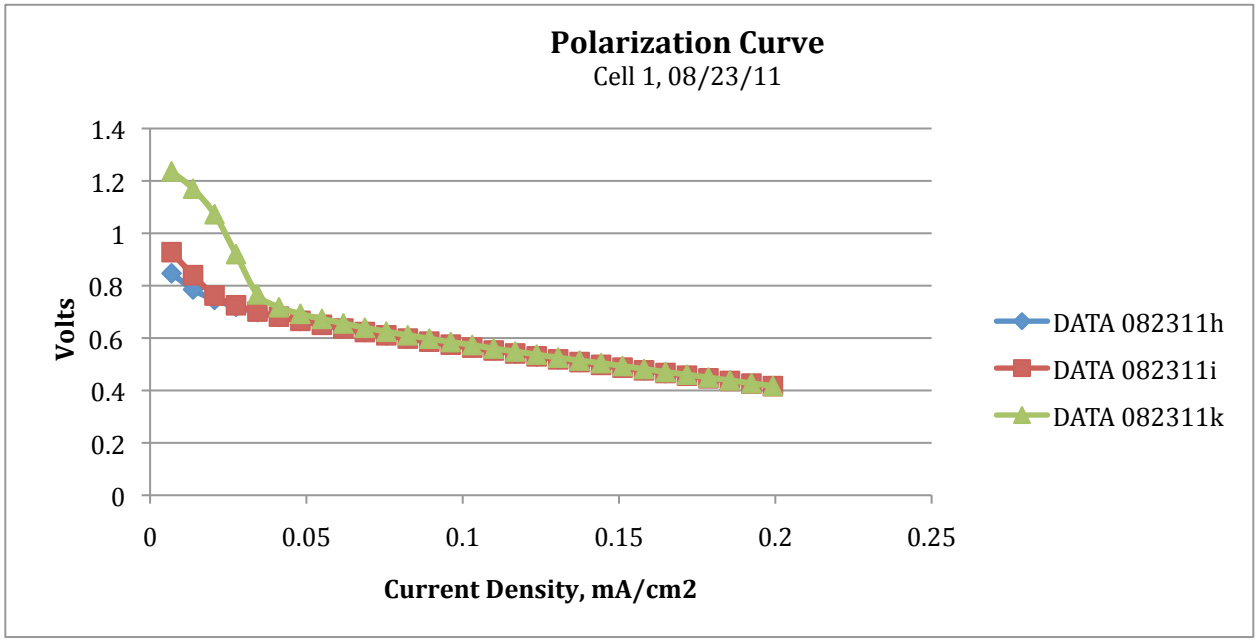

Figure 23 Polarization Curve for First Prototype Cell

The first prototype cell had the proper open circuit voltage and was rechargeable, but its current density was disappointing at only 0.2 mA/cm^2 as shown in Figure 23. A second prototype cell had lower performance due to possible incomplete conversion of the MEA from chloride form to hydroxide form and poor adhesion of the layers. The two cells differed in only one way, the thickness of the anode layer.

CONCLUSIONS

There are several technical issues affecting performance. The main technical issue is most likely that the gas diffusion layer (GDL) wetproofing is not withstanding the

chloride-to-hydroxide conversion process. Therefore, the GDL is filling with water which creates a diffusion barrier layer. The oxygen has to diffuse through this layer to react at the cell surface. Normally these pores are open to gas flow and the porosity is typically 70%. Improved performance is observed when the air backpressure is increased which forces more oxygen to the membrane (see blue polarization curve below where air pressure is increased to 5 psi temporarily). When the air pressure is released, the performance degrades back to the original slope.

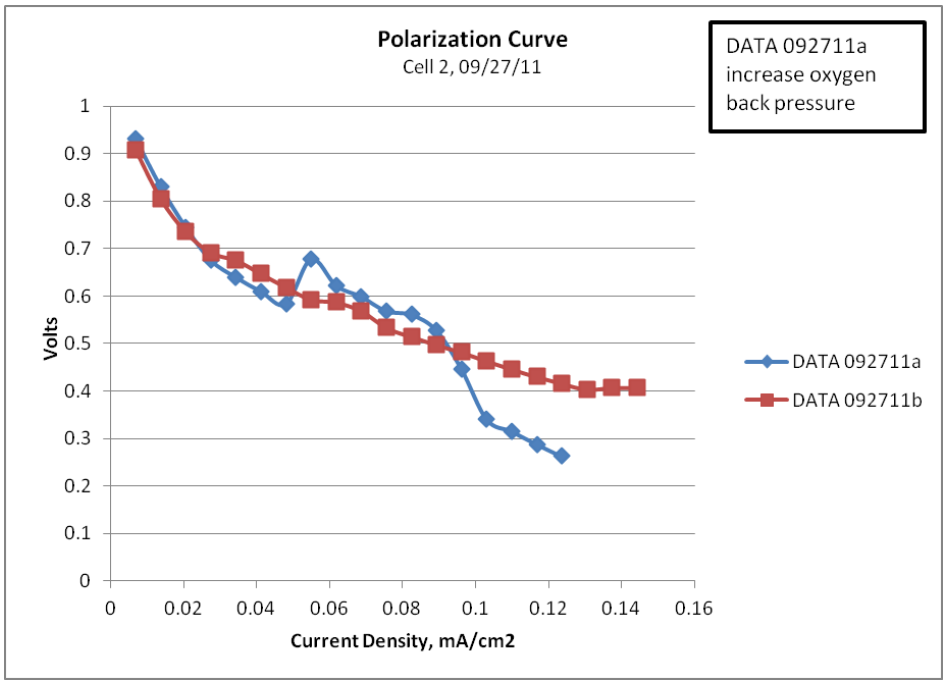

Figure 24 Cell 2 performance with test to show gas diffusion layer inhibiting performance.

Another technical issue is high cell resistance due to both chemical and physical characteristics. Future changes are to improve the casting and drying processes of the anode to make the zinc layer flat and of uniform thickness. Other avenues to investigate are the bonding of the electrodes to the membrane, sintering the nickel gas diffusion layer, and modifying the recipe to change resin or chopped fiber percentages.

The cell was charged on several occasions at varying voltages and time using a standard power supply. The best results were obtained when the voltage was dialed up to over 2 volts (approx. 2.25V) for approximately 1 hour. This puts the cell in electrolysis mode. The bifunctional catalyst was selected to have a lower overpotential so that it would not catalyze the oxidation of the nickel, although this could happen at higher current densities. The cell potential climbed from 0.8 volts to 1.6 volts and quickly dropped to about 1.25 volts when the power was removed.

The curves in Figure 25 show the low initial performance (blue line – DATA 102011a) and the recharged performance (red line – DATA 102011c). Also note the

green (DATA 102011d) and purple (DATA 102011e) lines which represent the steadily declining performance over the course of the day.

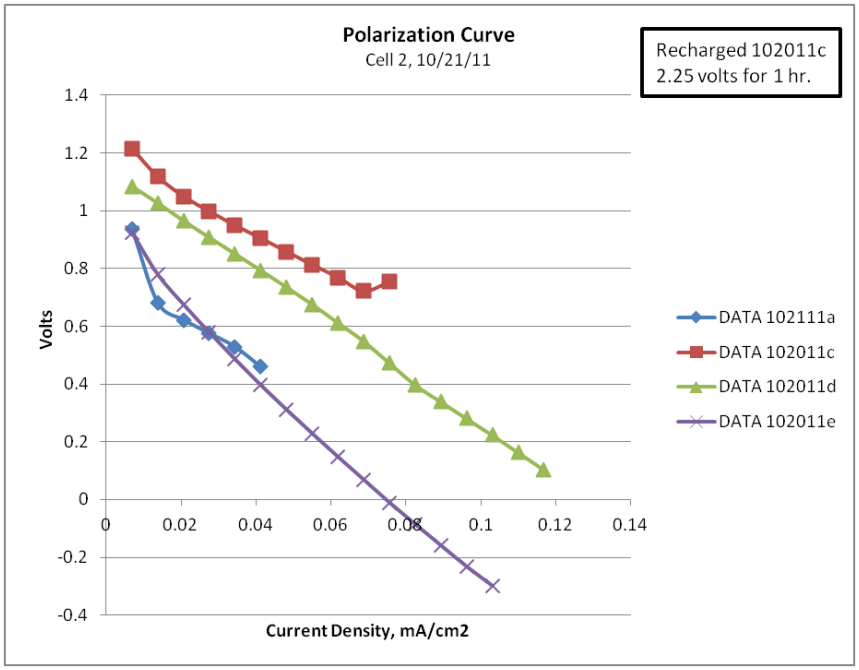

Figure 25 Multiple recharges on cell 2.

As a very first attempt with no prior experience manufacturing the electrodes, the prototype cell was rechargeable. Now the main challenge is to refine the manufacturing process to increase current density.